Mon. Not. R. astr. Soc. (1974) **169**, 477–526.

OBSERVATIONS OF 48 EXTRAGALACTIC RADIO SOURCES WITH THE CAMBRIDGE 5-KM TELESCOPE AT 5 GHz

G. G. Pooley and S. N. Henbest

(Received 1974 July 30)

SUMMARY

The 5-km telescope at Cambridge has been used to map 48 extragalactic radio sources at 5 GHz with an angular resolution $2'' \times 2''$ cosec δ. The results are presented here, together with various physical parameters derived for the sources.

1. INTRODUCTION

As part of the continuing programme of studies of extragalactic radio sources, we present here results of observations of 48 sources with the 5-km telescope at the Mullard Radio Astronomy Observatory. The instrument has been described by Ryle (1972); it is an Earth-rotation synthesis system at present operating at 5 GHz. At this frequency it has a synthesized response $2''$ in right ascension by $2''$ cosec δ in declination (measured between the half-power points). It is also used as an astrometric instrument for those sources which are not substantially resolved. The positional calibration is discussed by Ryle & Elsmore (1973).

Some of the sources described here were observed for the astrometric programme but were found to have too large an angular size; others form part of a study of a representative sample, or were suggested by Dr H. Spinrad in connection with his optical studies. Most have angular sizes in the range $2''$–$30''$, and they cannot be considered a complete sample for statistical purposes.

2. THE OBSERVATIONS

The eight elements of the telescope are connected to provide 16 independent interferometer spacings, with a maximum of 4·6 km. A single 12-hr observation is then sufficient to map a region of diameter $40'' \times 40''$ cosec δ. Most of the sources included in the present paper were mapped in this way; a number of the more extensive sources have been observed with two positions of the mobile aerials, giving 32 interferometer spacings and a clear field of twice the diameter.

The computation of the maps, which is carried out during the observations themselves, uses data weighted as exp $(-s^2/s_0^2)$, where s is the aerial spacing and s_0 is chosen so that the weight at the maximum spacing falls to 0·3. This grading function is chosen as a compromise between the best possible resolution and an acceptable sidelobe level; the observed response pattern is shown in Fig. 1, where it can be seen that the first and second sidelobes have amplitudes of -4 and $+3$ per cent, and are $2''$ and $3''$ from the maximum. The parameters for sources which are only just resolved have been established by examining the 16 interferometer records directly, since the information from the largest spacings is then used most effectively. The maps made with one 12-hr observation have an rms noise level of about 3 mfu (3×10^{-29} W Hz^{-1} m^{-2}); for maps made with two 12-hr observations, the noise level is about 2 mfu.

The main limitation to the operation of instruments of high resolution is the disturbance caused by atmospheric irregularities. Substantial phase variations are sometimes observed, and these are worse during summer daytime when the typical

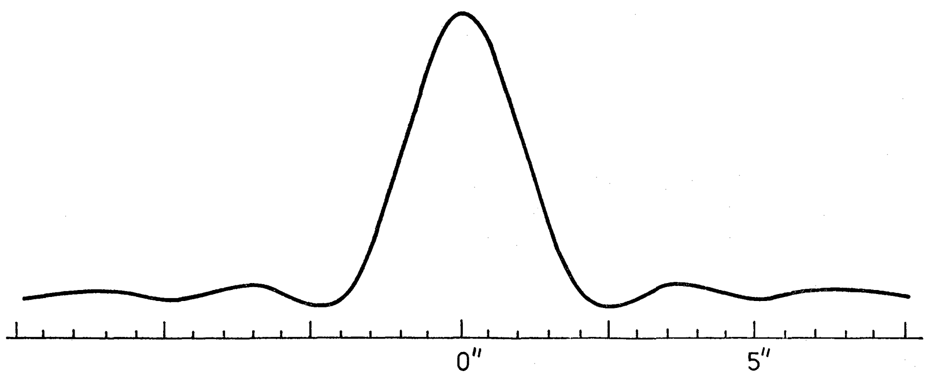

FIG. 1. *The synthesized response of the telescope in right ascension. The response in declination is similar but wider by a factor cosec δ.*

scale of the irregularities is about 0·7 km (Hinder & Ryle 1971). Larger scale features, 5–30 km in extent, are also found throughout the year (Hargrave & Shaw, private communication). The principal consequence of the latter irregularities is the introduction around each source of radial sidelobes, the presence of which is usually easily recognized. Any run seriously affected in this way was repeated, and it is thought that none of the maps is in error by more than about one contour as a result of atmospheric irregularities.

Each source (with the exception of 3C 304 and those from the 4C catalogue) has been mapped twice: once with the linearly polarized feeds parallel (*E* vector in p.a. 90°) and once with the feeds of the moving and fixed aerials orthogonal, to measure the linear polarization. During the polarization observations the feeds were rotated to each of four position angles, separated by 45°. The polarization observations give maps representing the Stokes' parameters *Q* and *U*, which were then combined to determine the position angle and intensity of the linear polarization. No attempt has been made to measure the circular polarization of the sources. The parallel-feed observations give maps representing *I–Q*; the observations of *Q* could of course be added to these to give the total intensity *I* but, since this involves a decrease in signal-to-noise ratio and since the polarization seldom exceeds about 10 per cent, this procedure has not been adopted. The remaining sources were mapped with parallel feeds only.

The maps themselves are presented in Fig. 2. Each one shows *I–Q*, and the intensity and direction of the linear polarization (*E* vector) where this is significant. One detail of the presentation should be noted particularly: for most of the sources, the map has been compressed by a factor cosec δ in declination, a convention which makes the telescope response circular and therefore assists in the interpretation of partially resolved components. A few maps, of well-resolved sources, are not compressed in this way. Note that the position angles of the *E* vectors appearing on the maps are always the true position angles, not modified by the compression, and so the relationship between the source structure and the magnetic field

(*Continued on p.* 510)

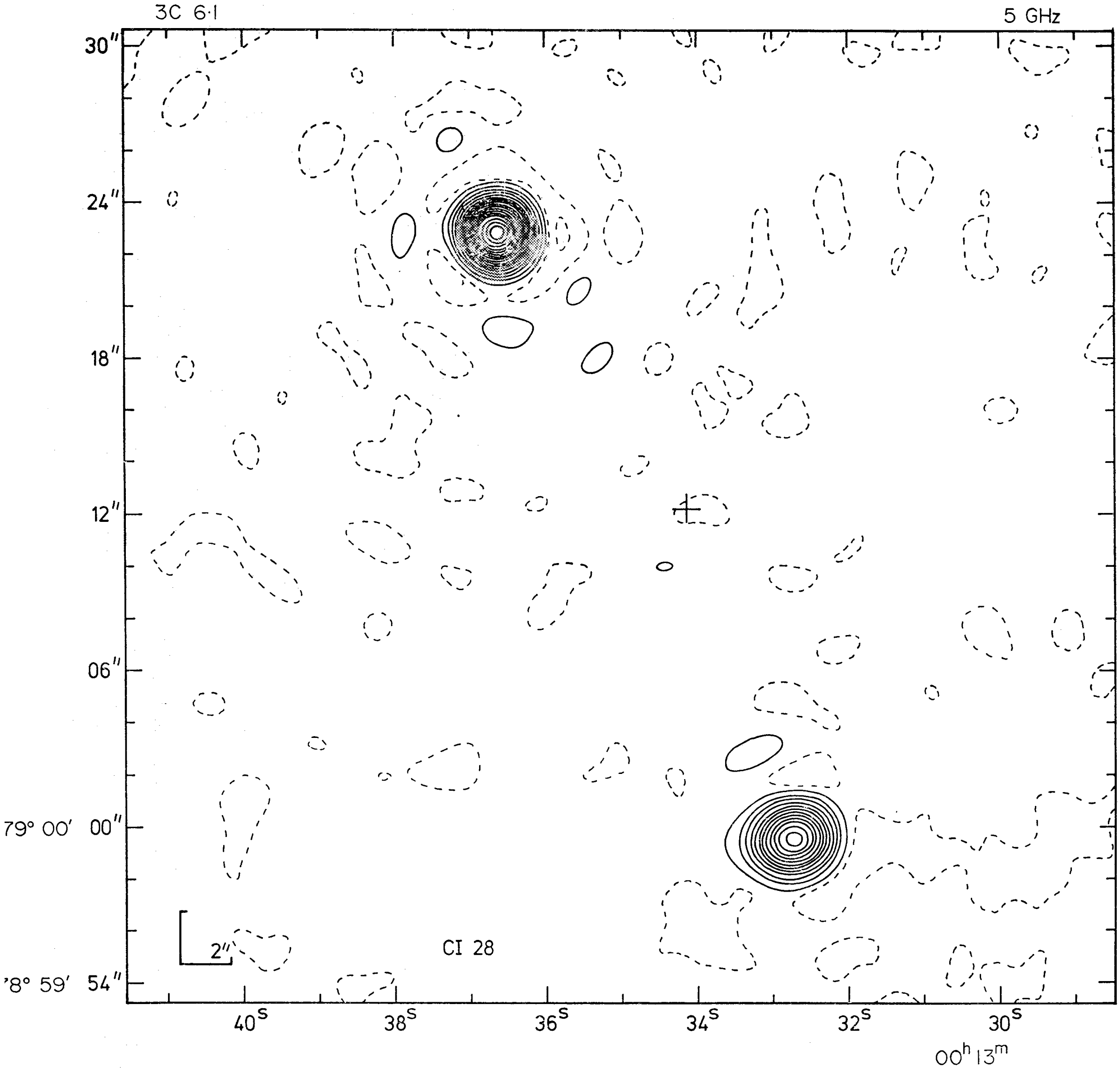

Fig. 2. 3*C* 6.1. *This source probably has a very weak central component. The cross marks the position of a* 23^{m} *object* (*GL*).

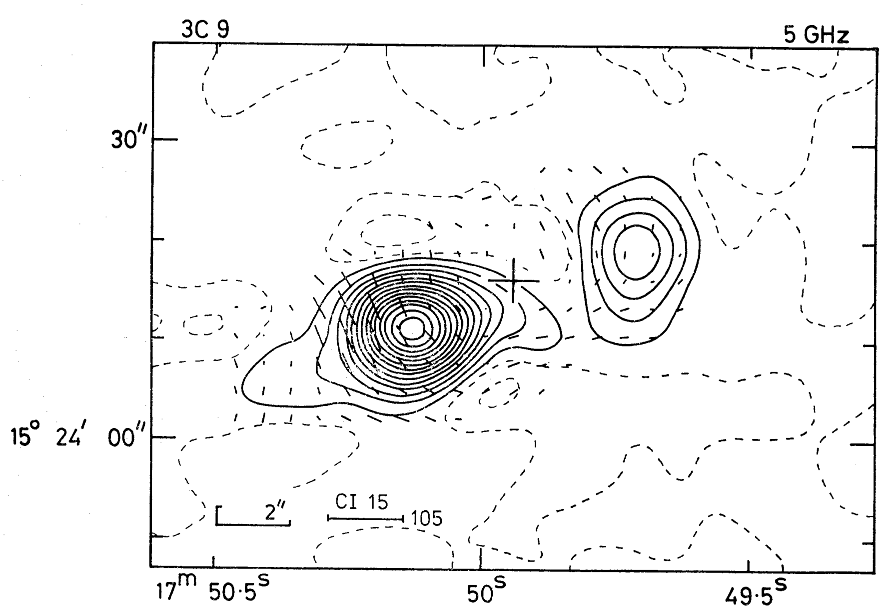

Fig. 2. 3*C* 9. *The cross marks the position of the* 18^{m} *variable QSO* (*AK, MTC*).

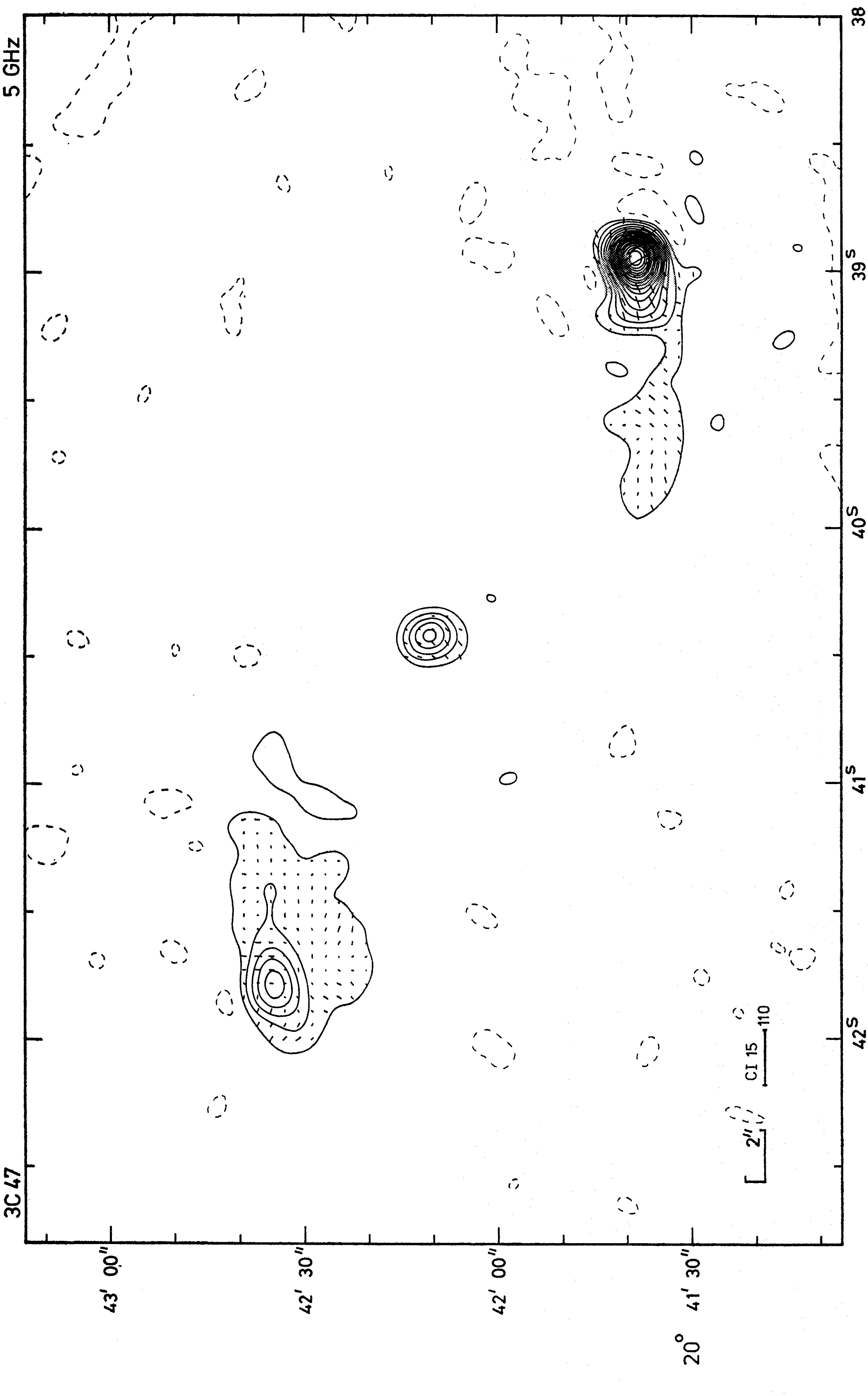

FIG. 2. 3C 47. *The optical position of the* 18m *QSO measured by BCGP lies* 1″·6 *from the central radio component. The Sf component*

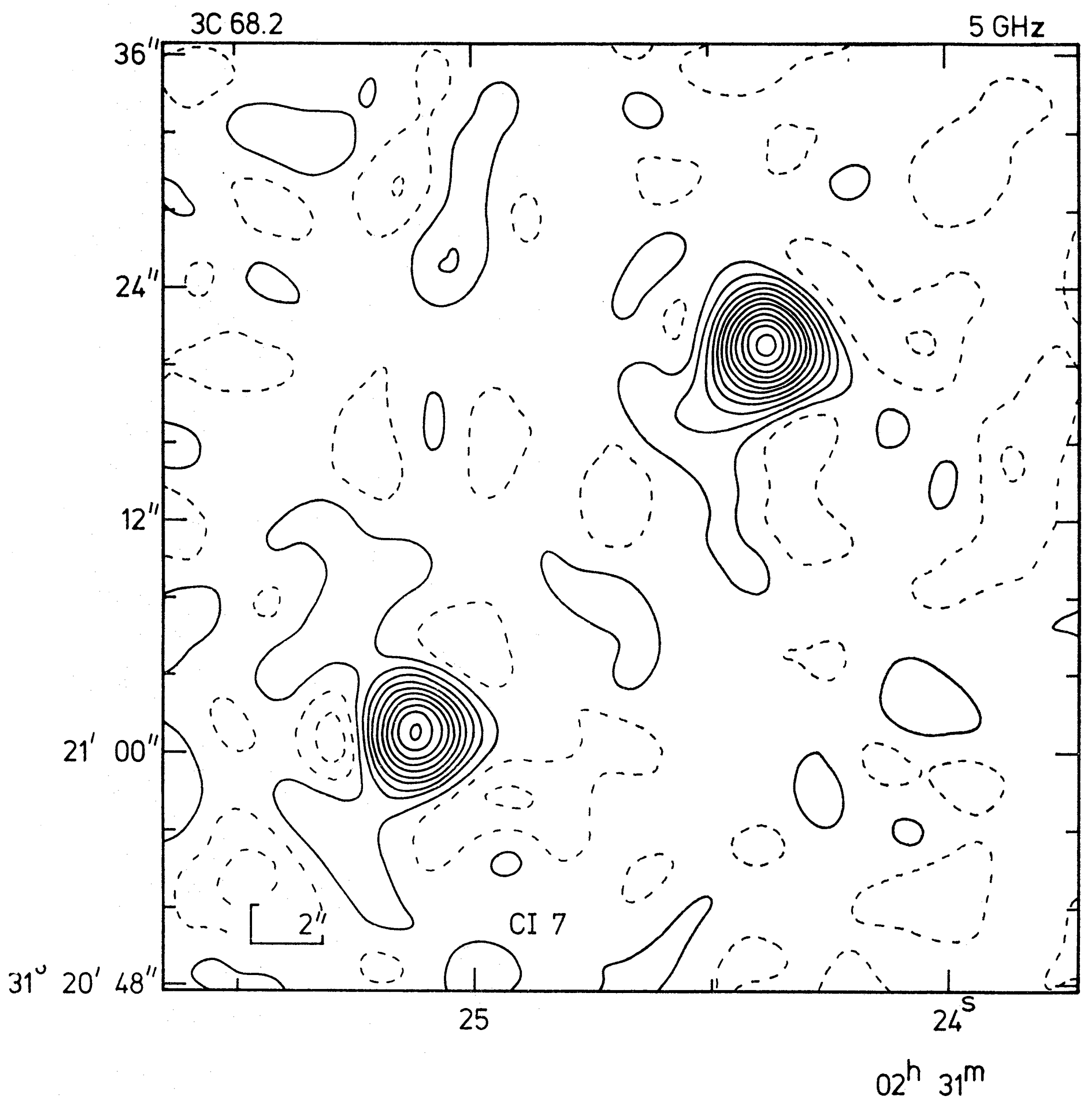

FIG. 2. 3C 68.2. *There is no optical identification* (*GL*).

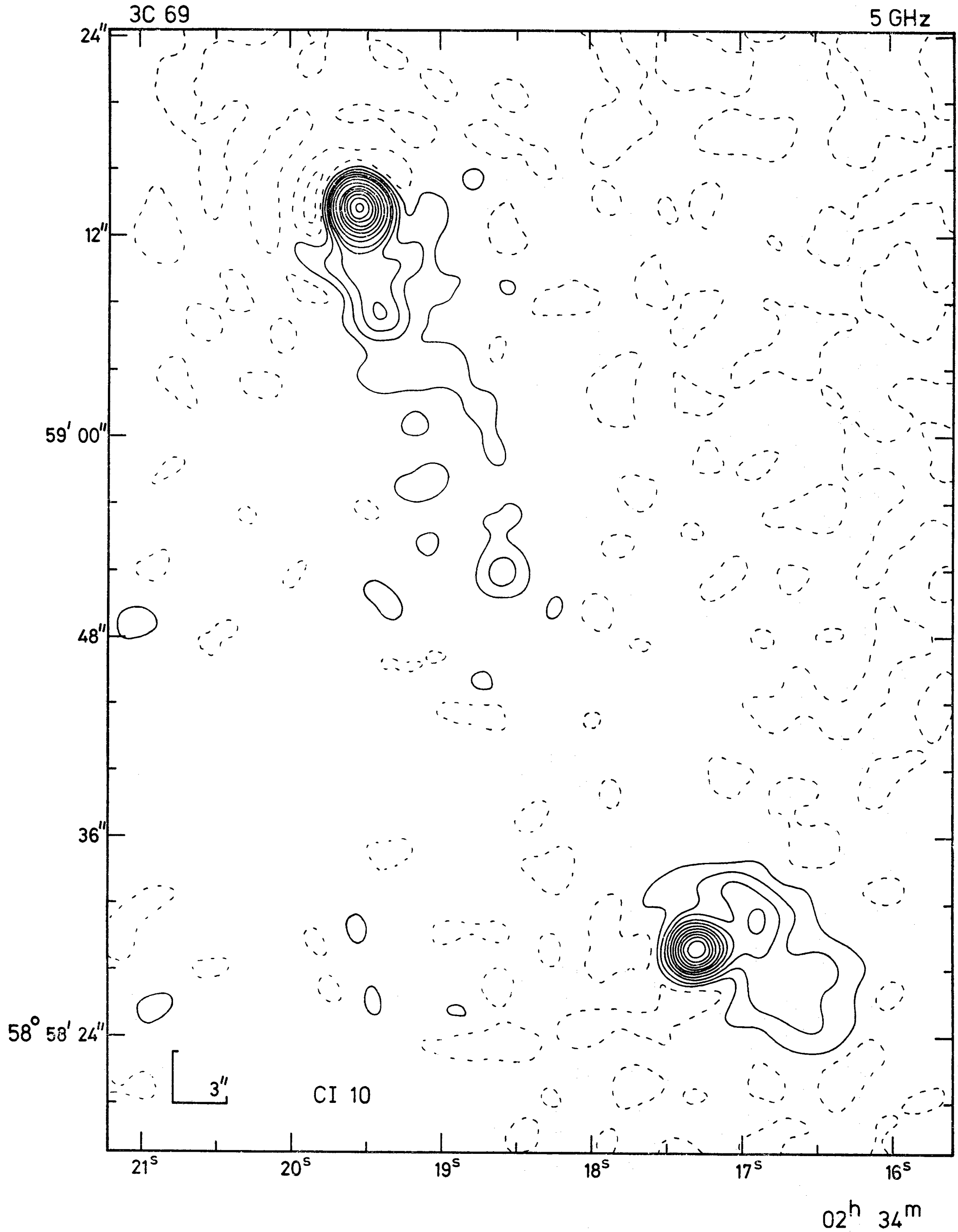

FIG. 2. 3*C* 69. *There is no optical identification. Alternate contours above No.* 5 *in the northern component have been omitted.*

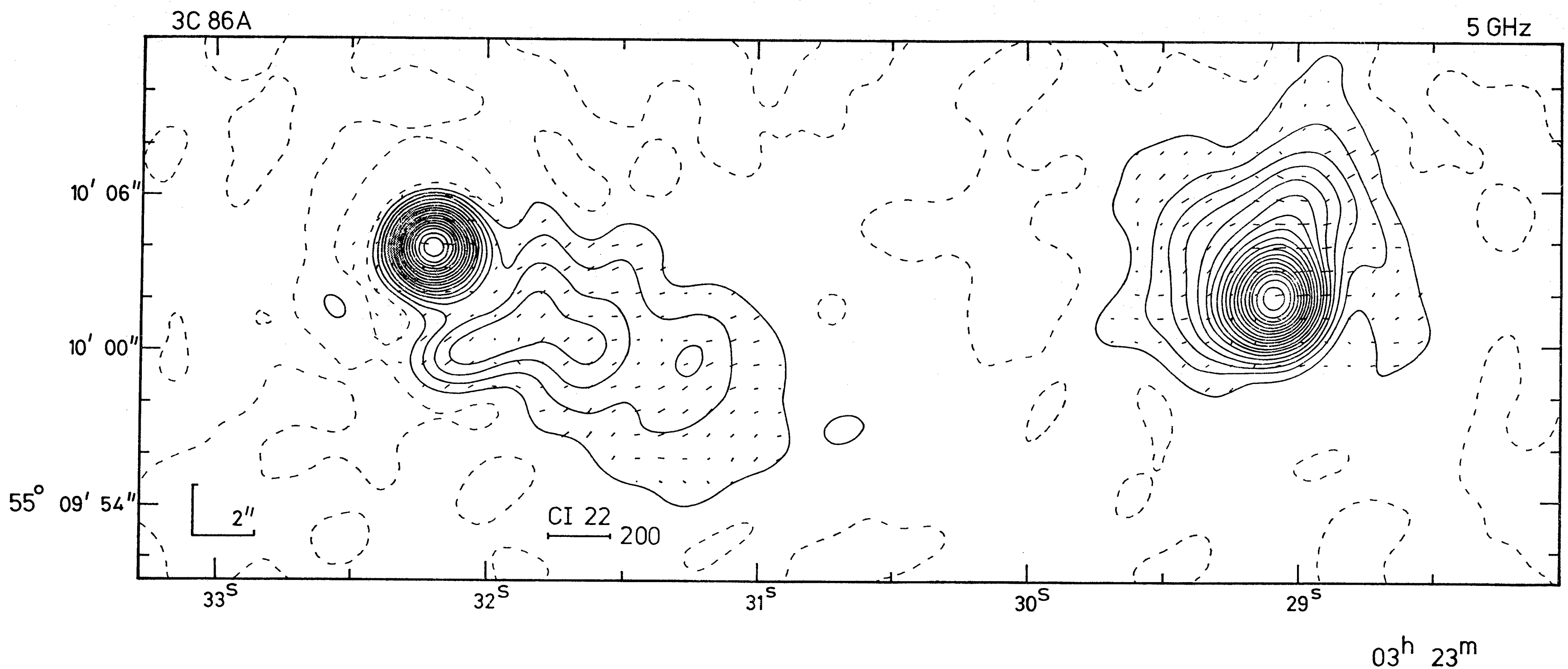

FIG. 2. 3*C* 86*A*. *The peak of polarization in the preceding component does not coincide with the maximum of total intensity. There is no optical identification. The unpolarized map has already been published* (*Ryle* 1972).

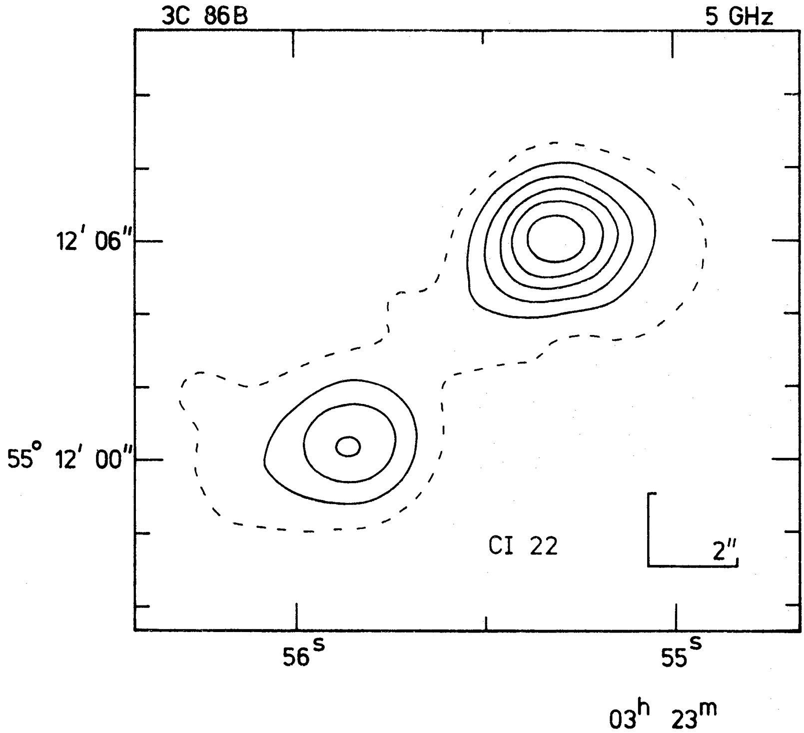

FIG. 2. 3C 86B. *There is no optical identification.*

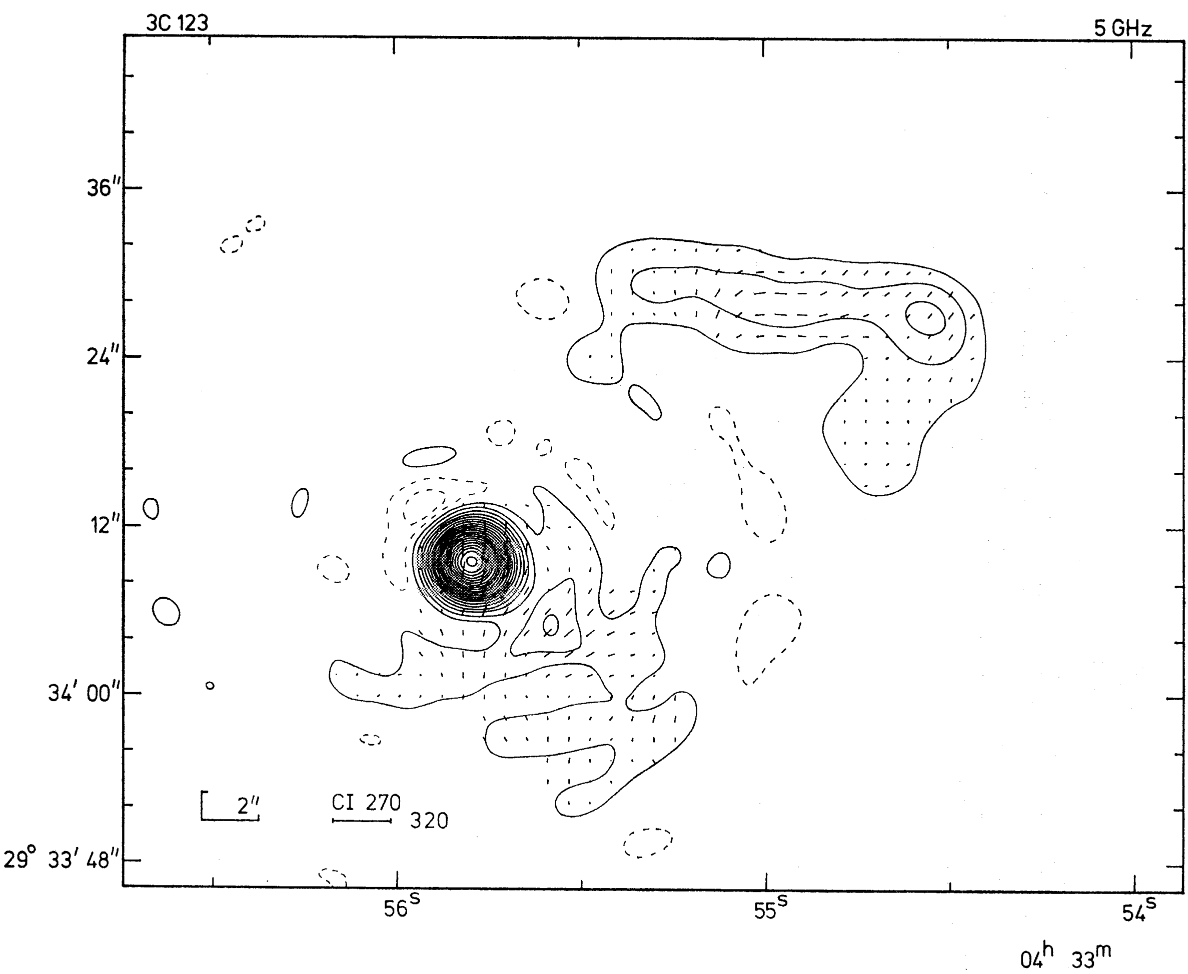

FIG. 2. 3C 123. *A* 20^{m} *galaxy lies near the centre of the source* (L).

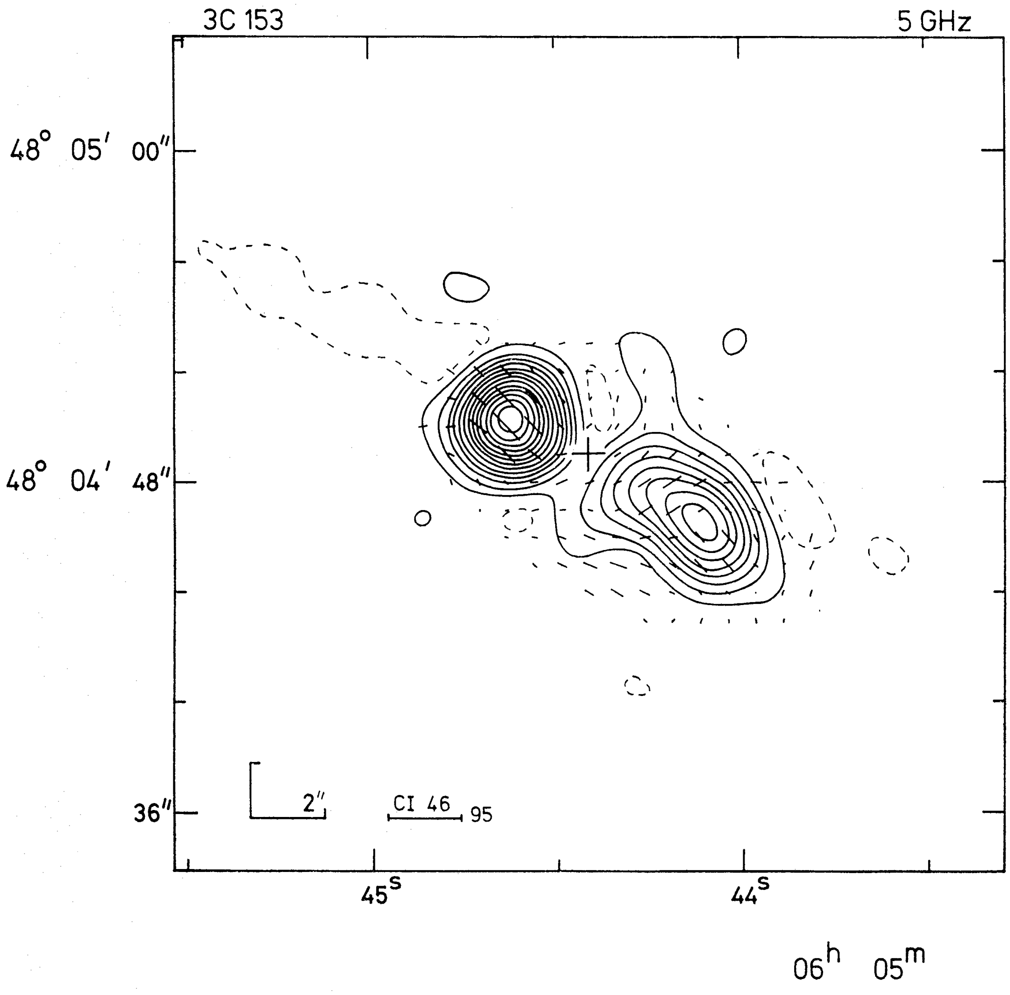

FIG. 2. 3*C* 153. *The position (AK, MTC) of a red galaxy in a cluster is marked.*

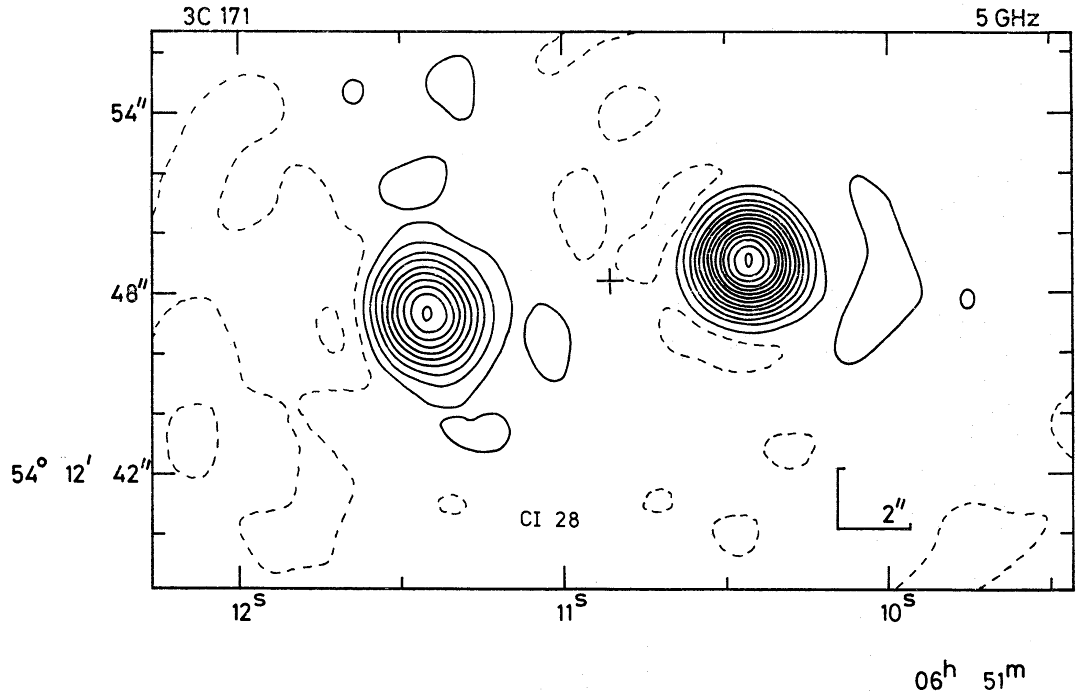

FIG. 2. 3*C* 171. *The position (WWD) of the* $18^m{\cdot}5$ *galaxy is marked. Sandage (1967) describes it as an N galaxy. Approximately 30 per cent of the radio flux originates in a region some 20″ in diameter, not represented here.*

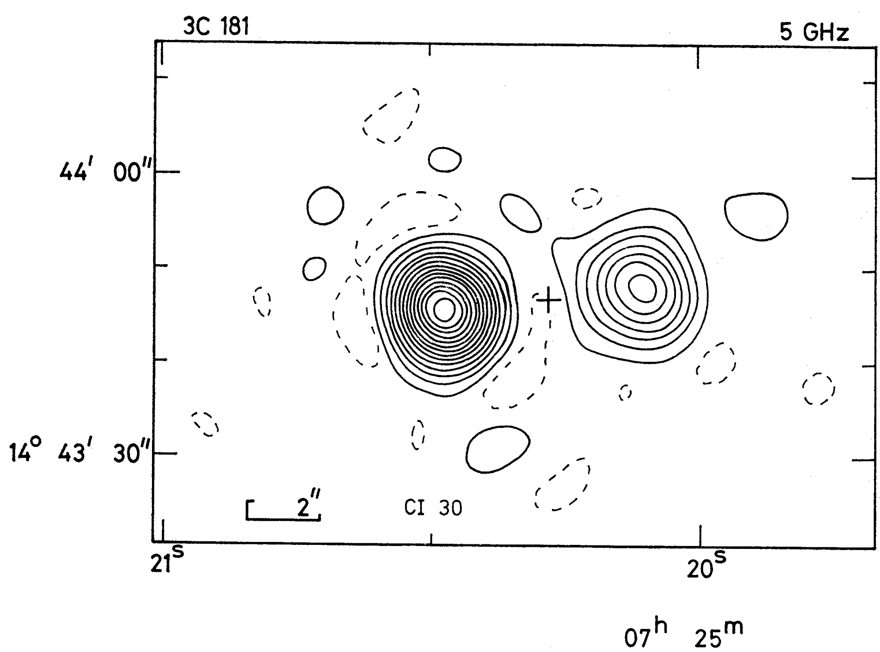

FIG. 2. 3*C* 181. *The variable* 19^m *QSO (WWD) is marked.*

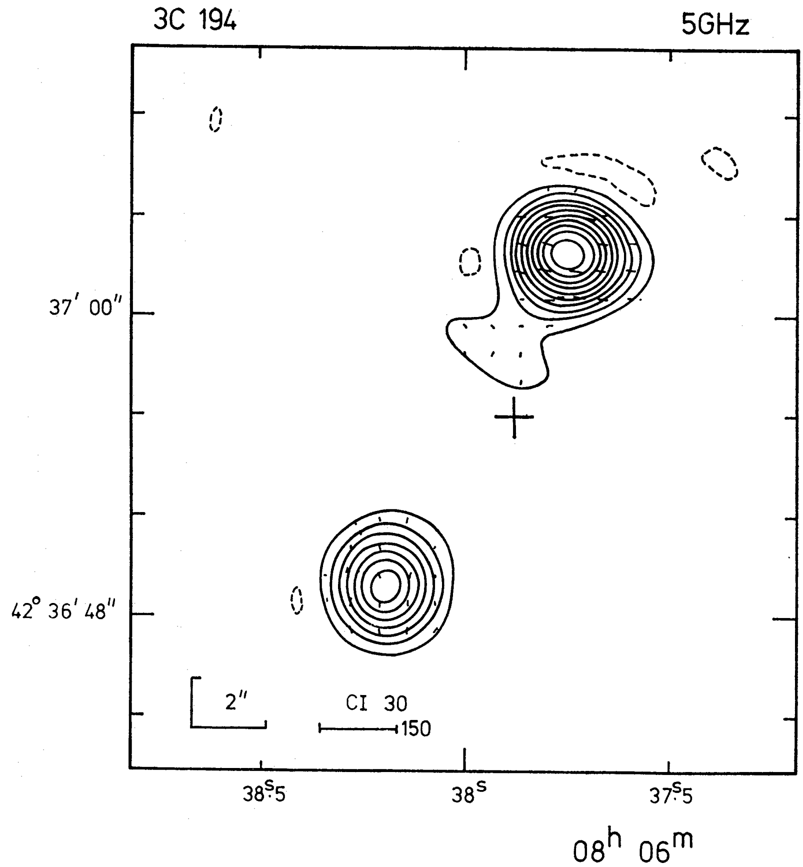

FIG. 2. 3*C* 194. *The position* (*Wlérick* et al. 1971) *of a* 20^m *red object is marked.*

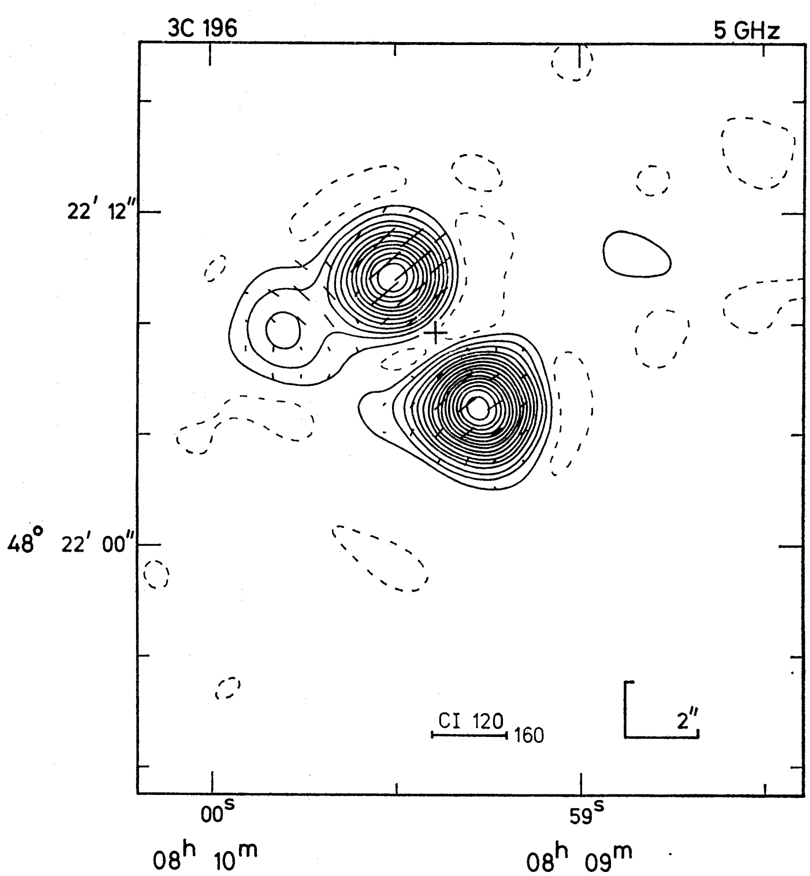

FIG. 2. 3*C* 196. *The variable* 18^m *QSO* (*AK, MTC*) *is marked.*

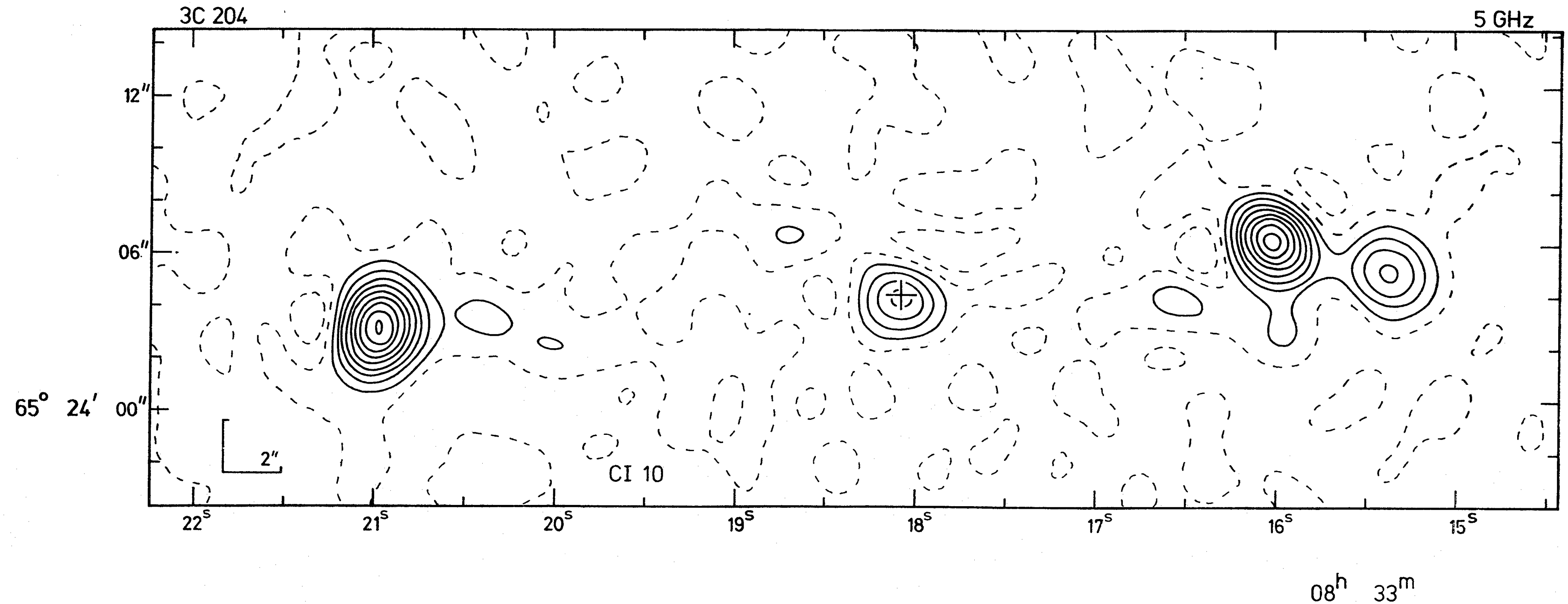

FIG. 2. 3C 204. *The central component coincides with the* 18m *QSO* (*AK*, *MTC*).

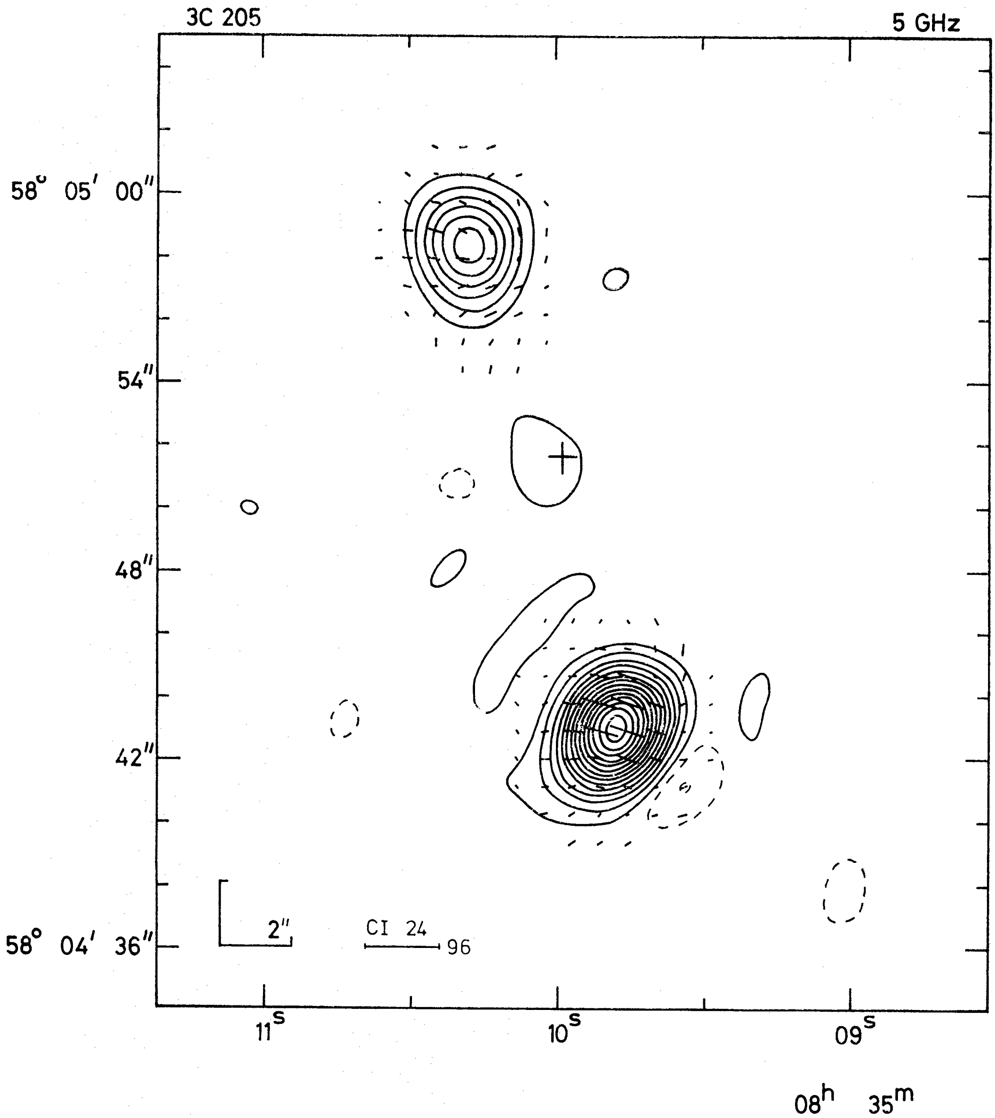

FIG. 2. 3*C* 205. *The* 18ᵐ *QSO* (*AK*, *MTC*) *is marked.*

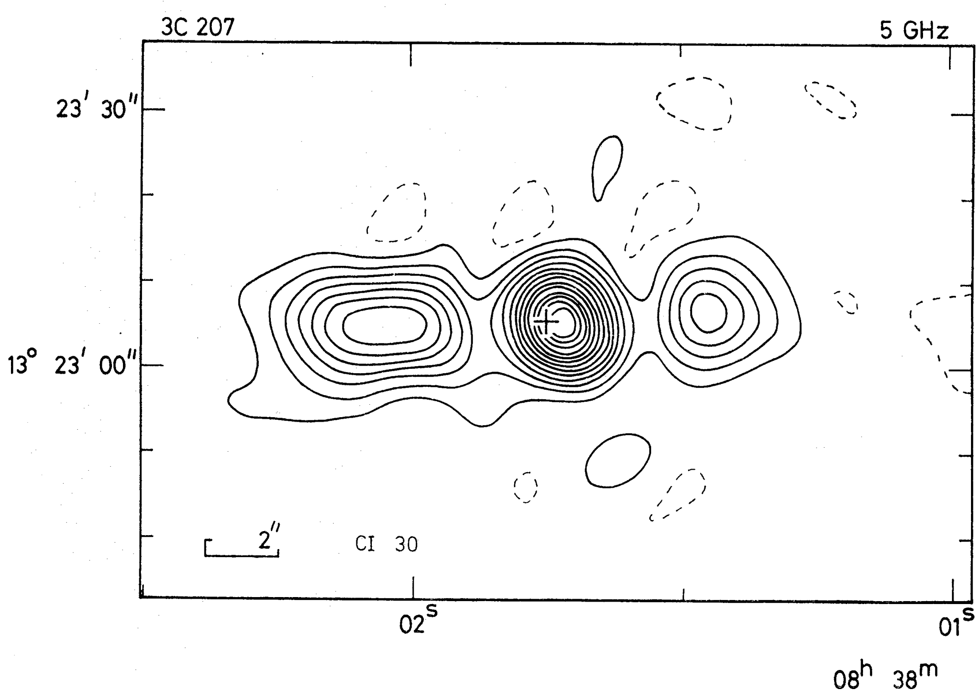

FIG. 2. 3*C* 207. *The* 18ᵐ *QSO* (*WWD*) *is marked.*

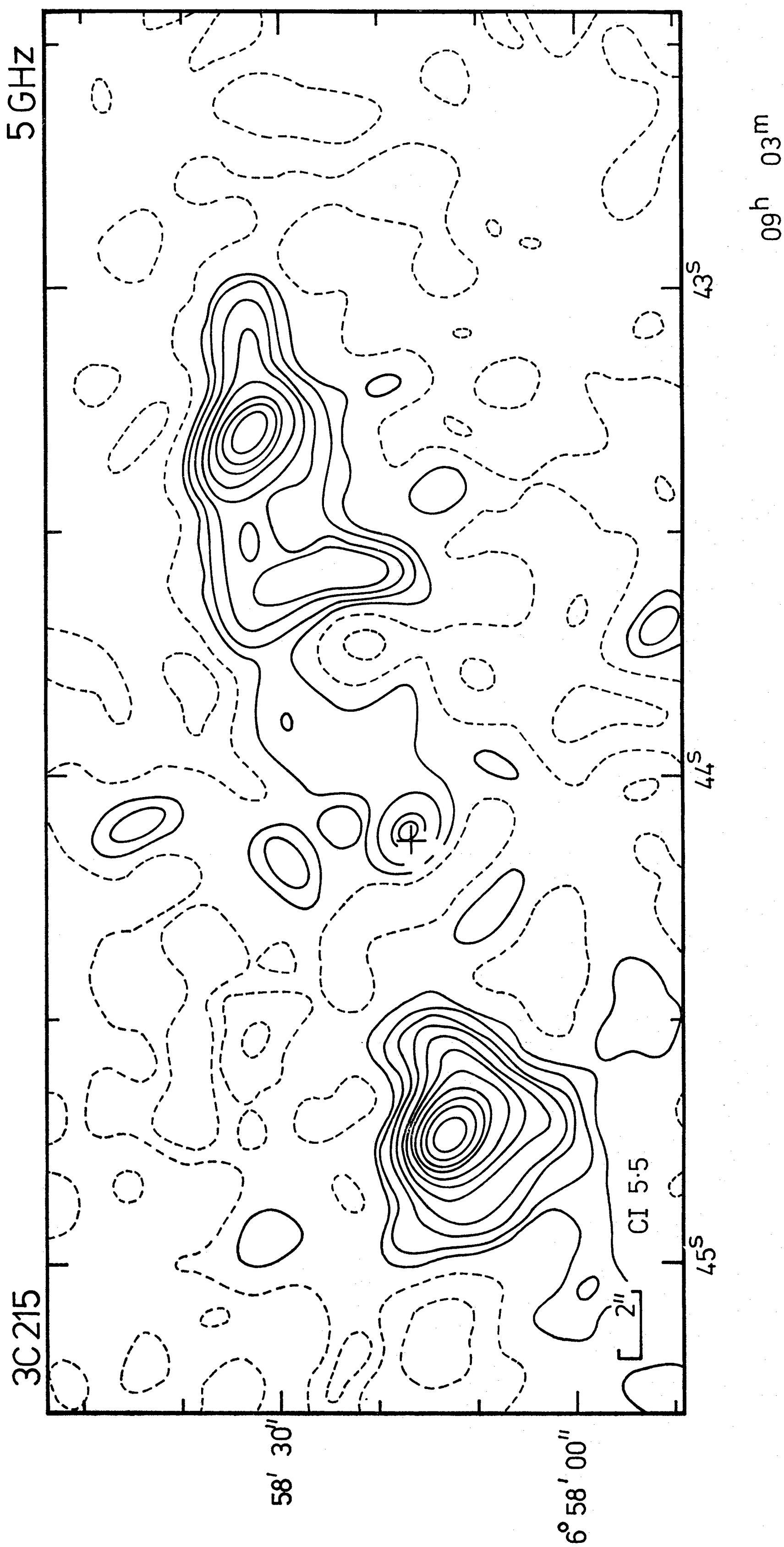

FIG. 2. 3C 215. *The position of the* 18^{m} *QSO* (*Hunstead* 1971; *Kapahi* et al. 1974) *is marked.*

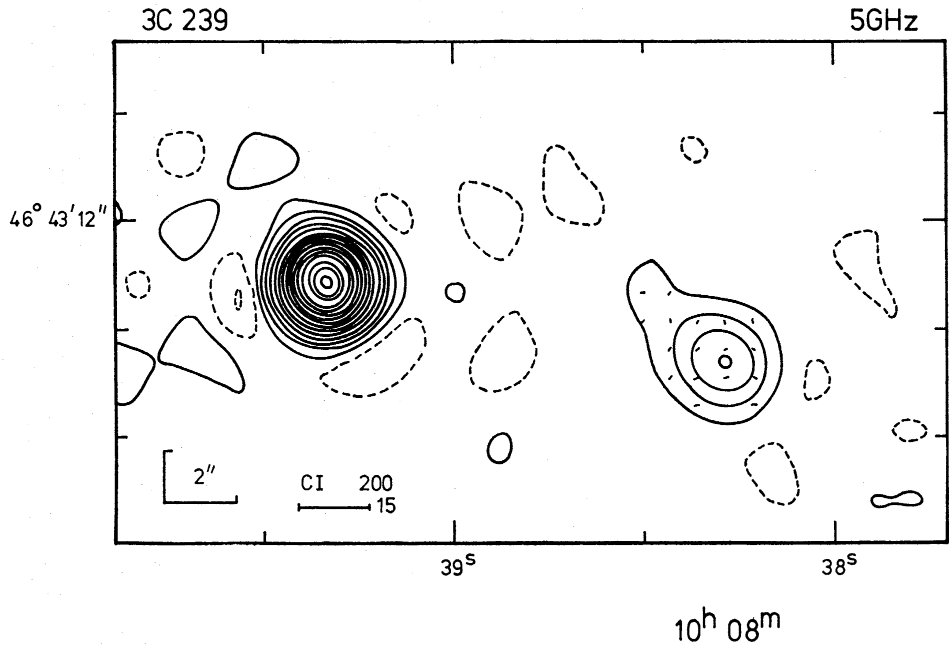

FIG. 2. 3*C* 239. *This source has been identified with a* 20^{m} *red galaxy in a cluster, but there is no accurate optical position.*

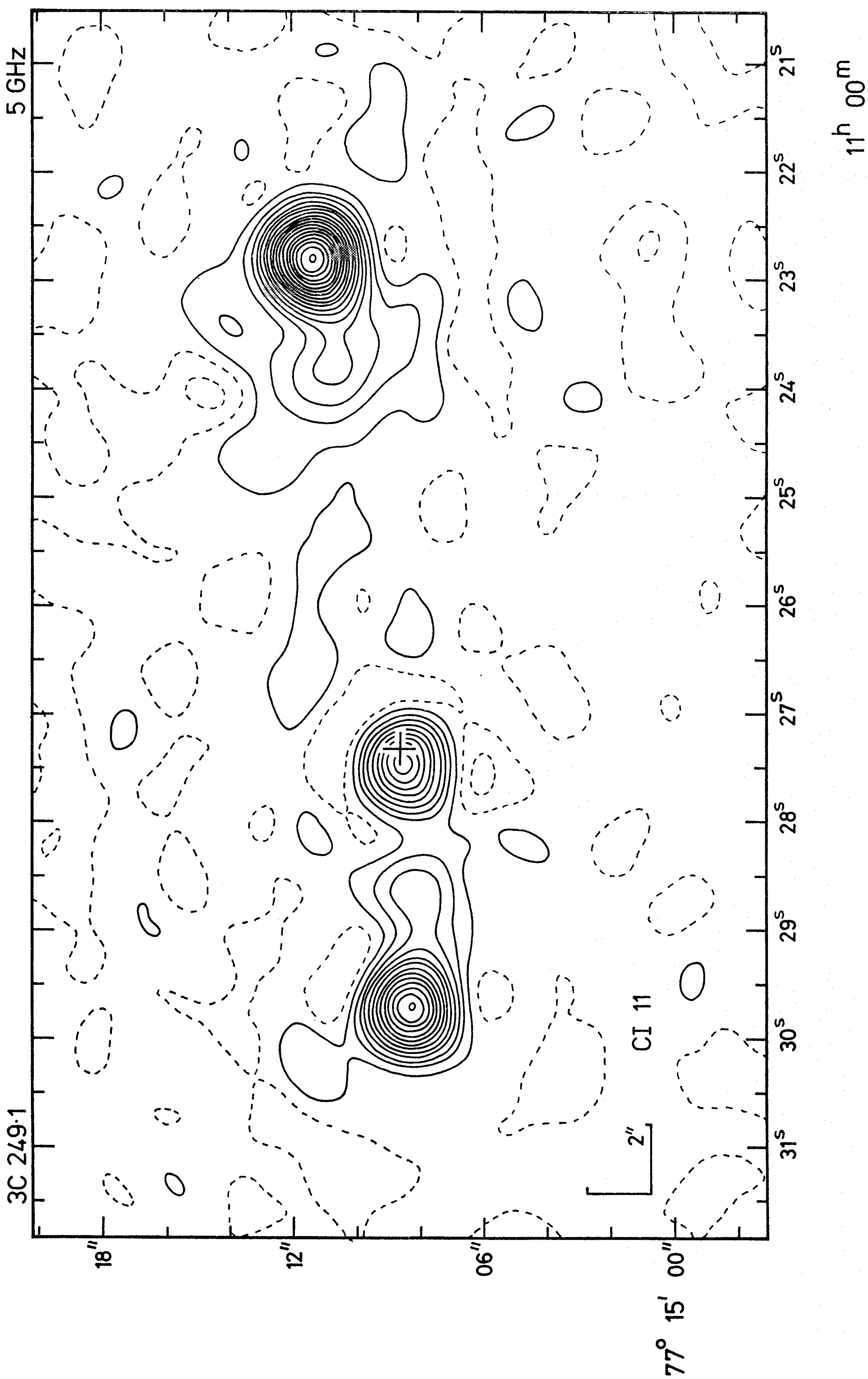

FIG. 2. 3C 249.1. *The position (AK, MTC) of the* 16^{m} *variable QSO is marked.*

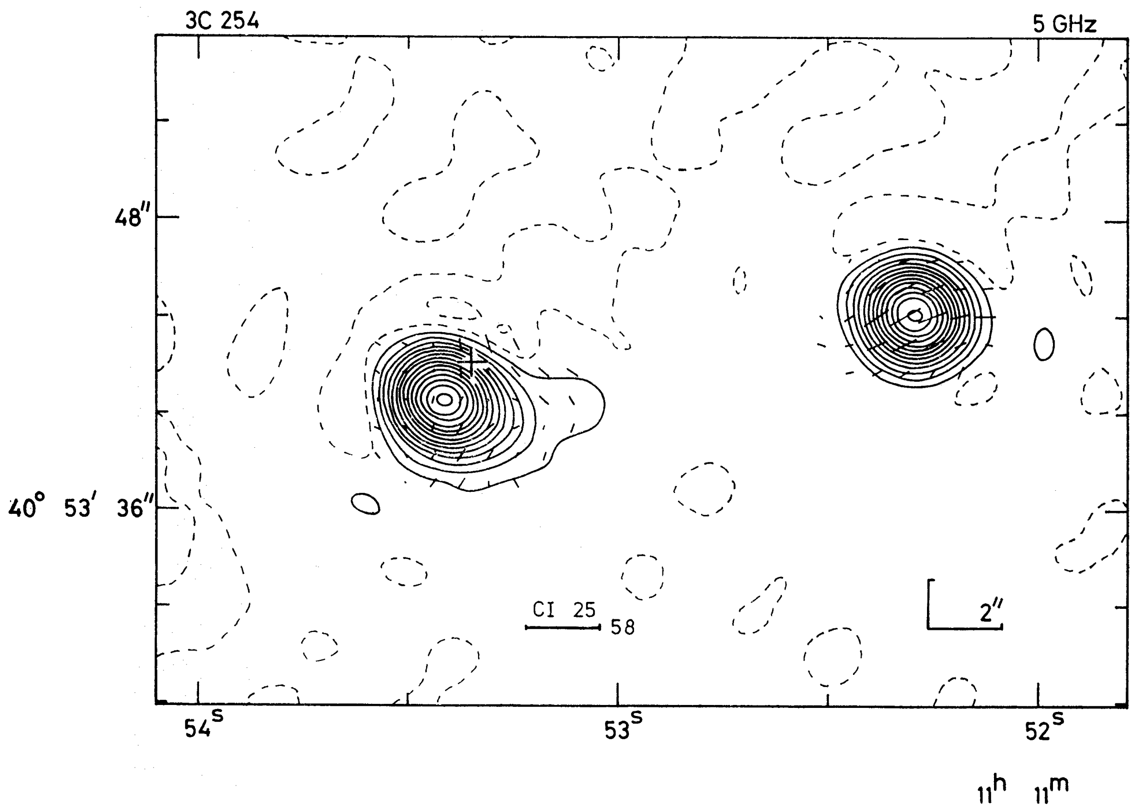

FIG. 2. 3*C* 254. *The position marked* (*G*) *is that of the* 18^{m} *QSO.*

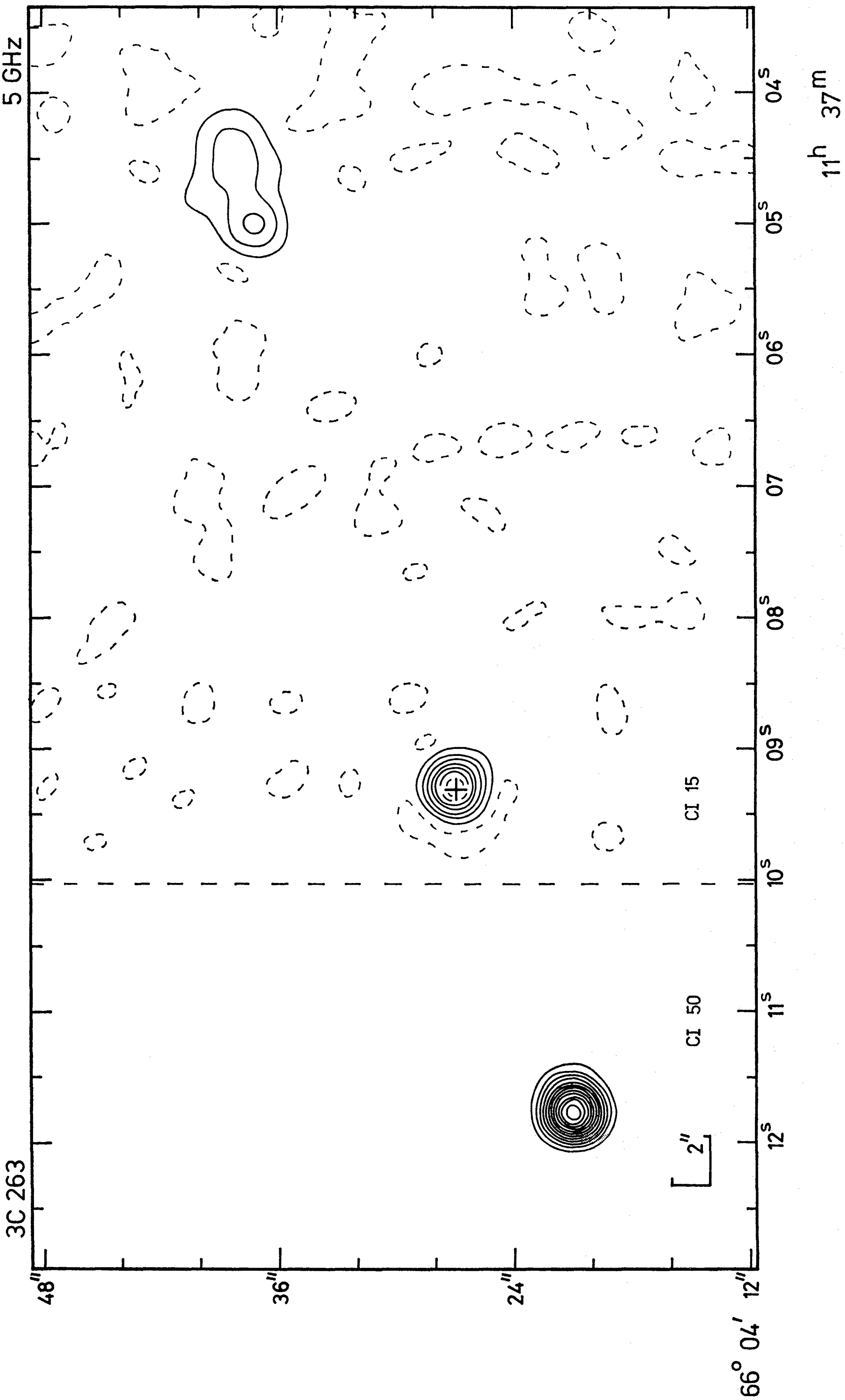

FIG. 2. 3C 263. *The position of the variable 16m QSO (AK, MTC) is marked. The ratio of intensities of the two outer components is 15 : 1, and two different contour intervals have been used.*

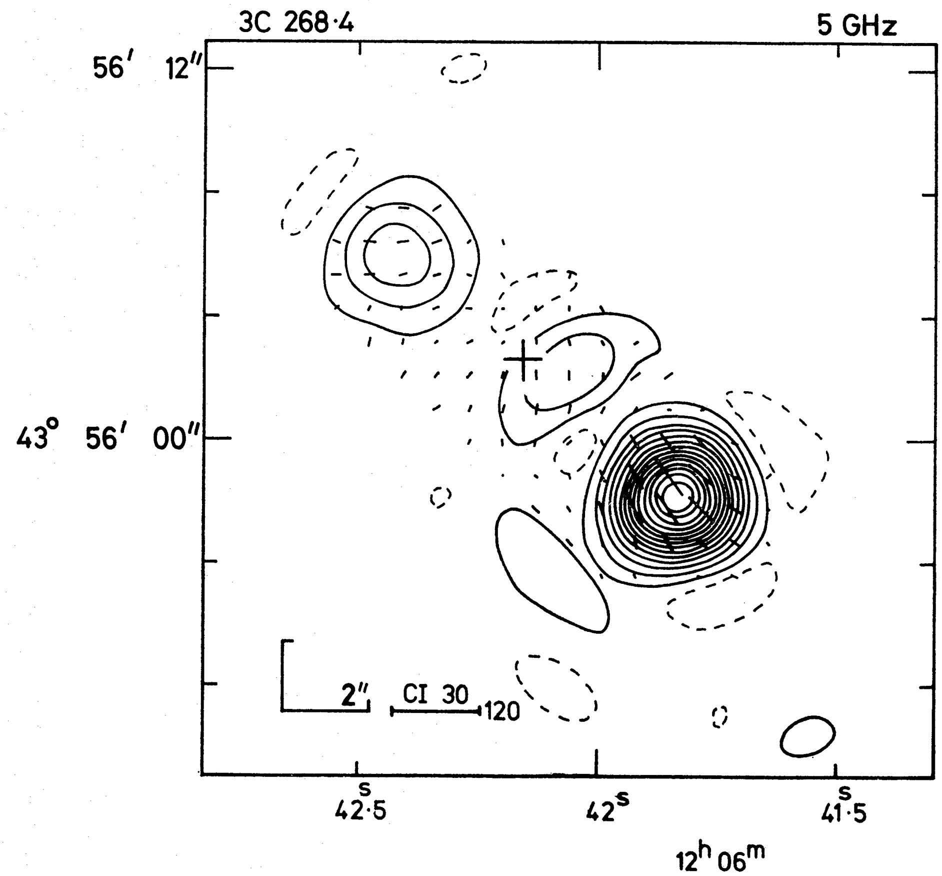

FIG. 2. 3*C* 268.4. *The position (V) of the variable* 18^{m} *QSO may coincide with the central radio component. Burbidge* et al. (1971) *note that this source lies only* 3′ *from the galaxy NGC* 4138, *but the radio structure does not suggest a real association.*

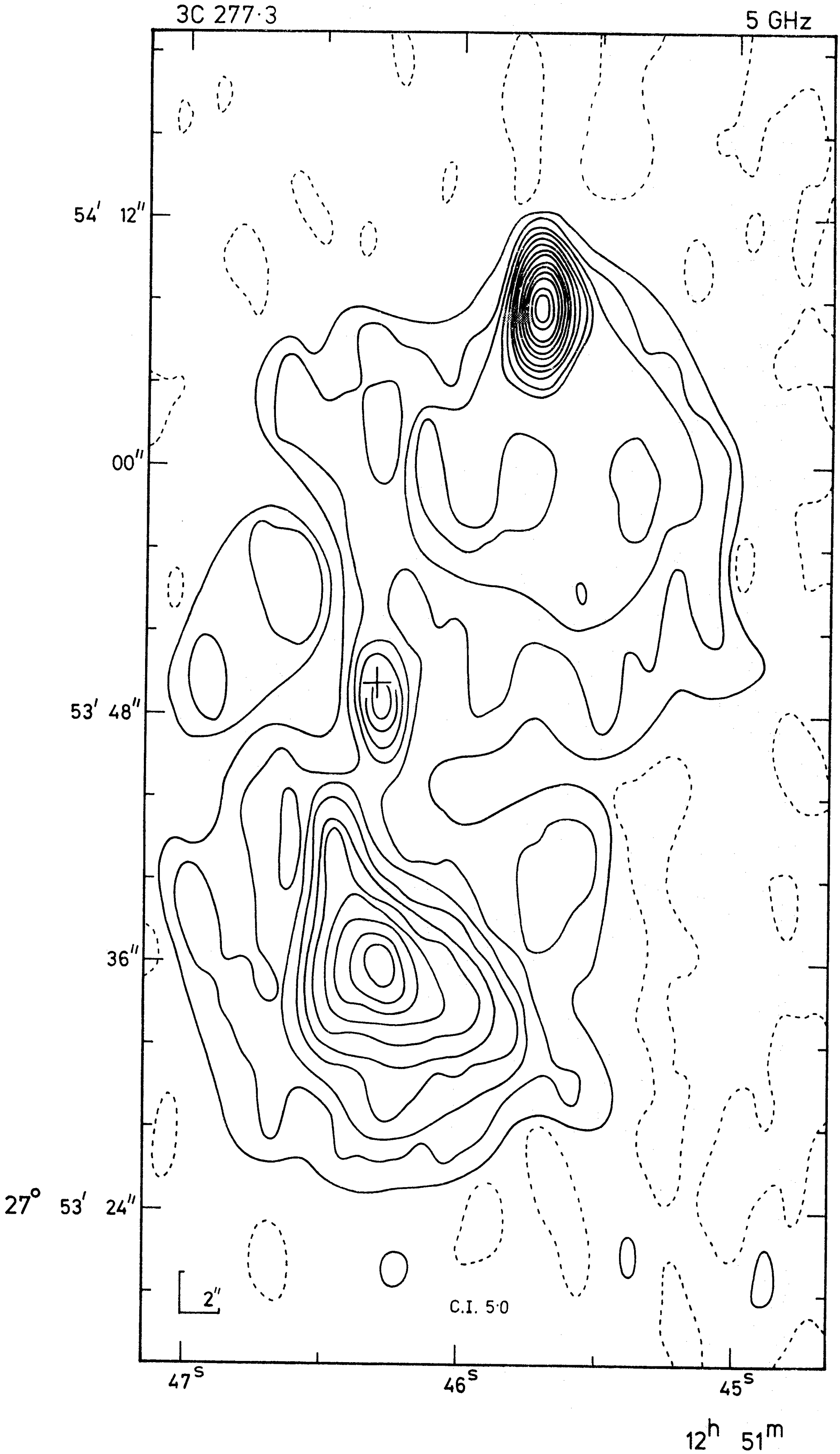

FIG. 2. 3*C* 277.3. *The declination scale of this map is not compressed. The position* (*G*) *of the nucleus of the* 15m *D*2 *galaxy is marked. Much of the radio source appears embedded in the optical galaxy.*

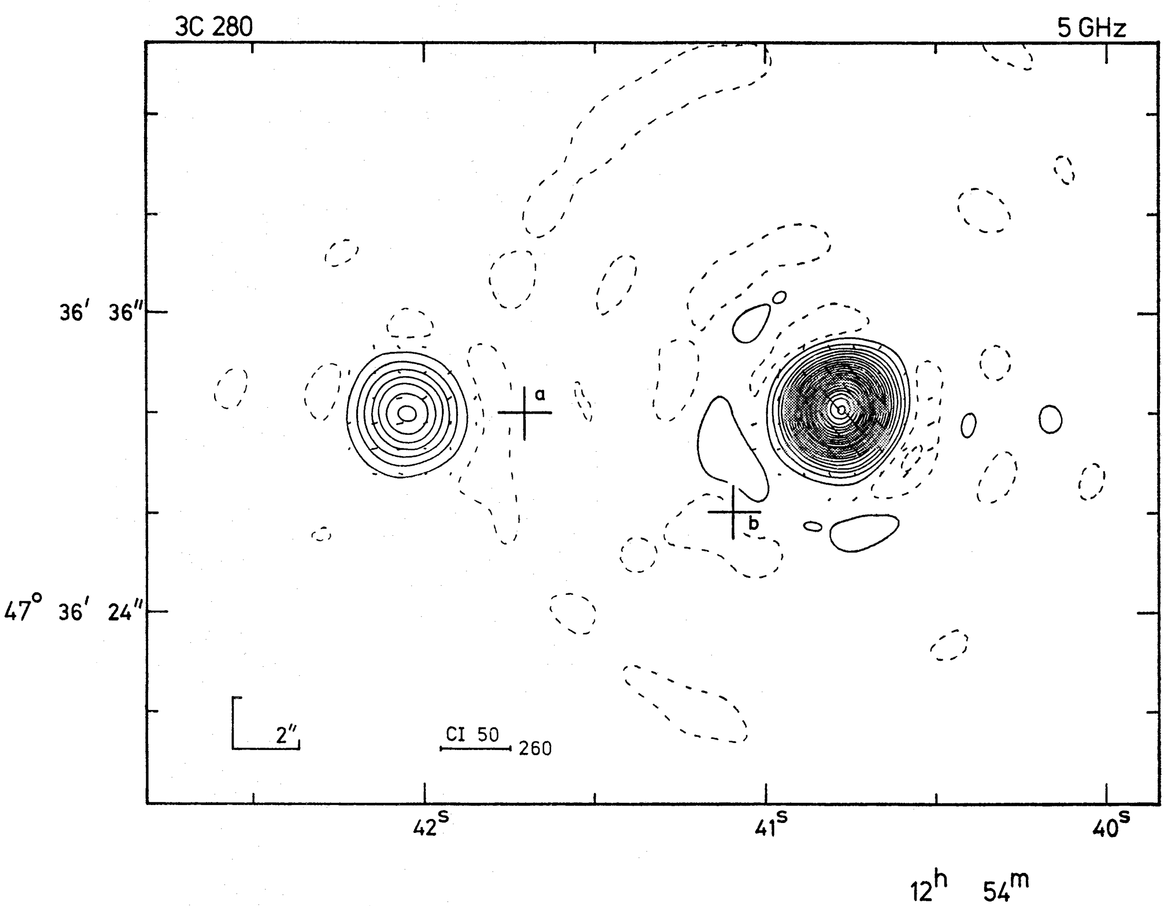

FIG. 2. 3*C* 280. *The positions of two very faint (≃22m) galaxies (KSK) are marked.*

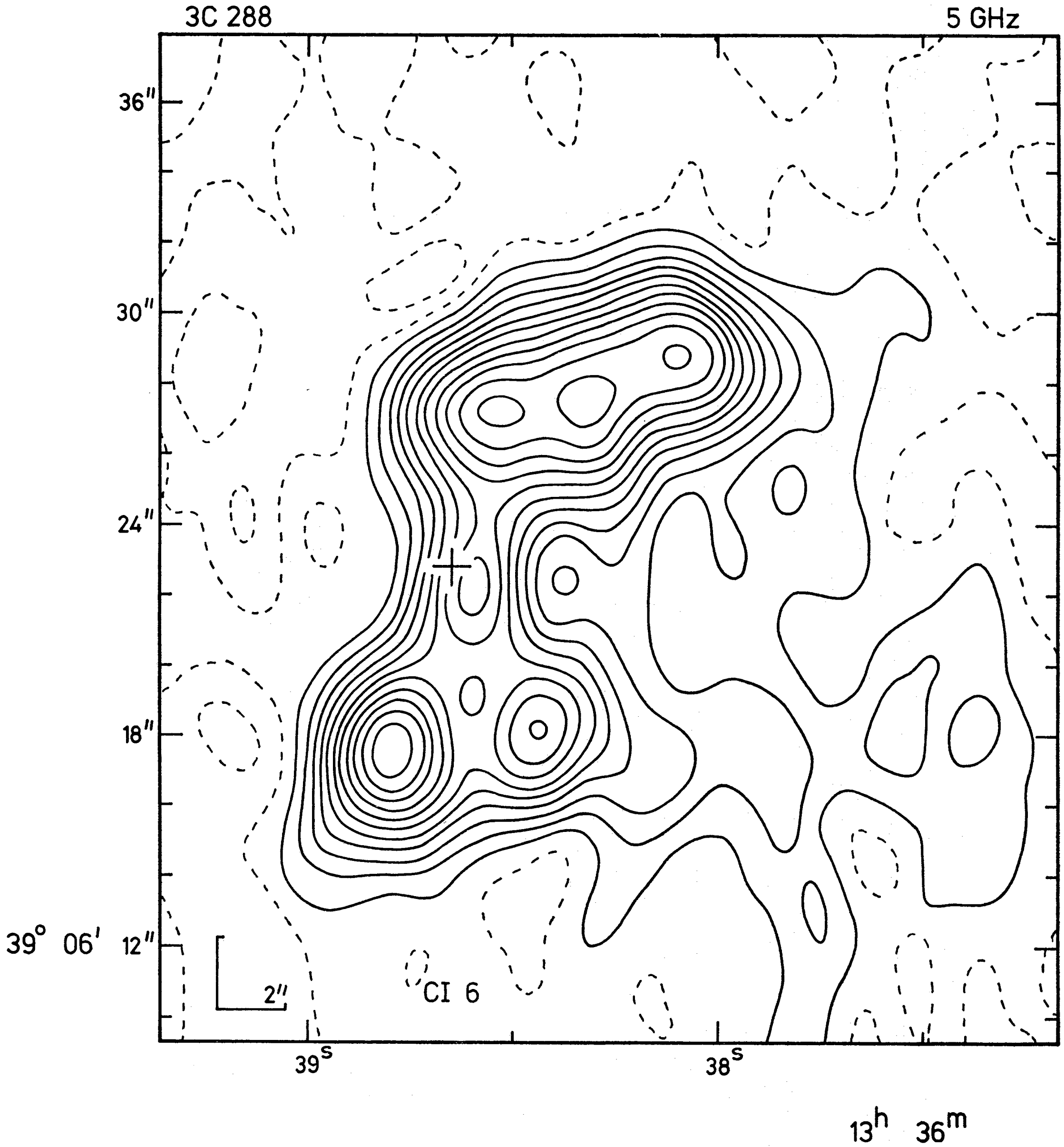

FIG. 2. 3*C* 288. *This map is not compressed in declination. The position* (*V*) *of the nucleus of the* 16ᵐ *D*4 *galaxy may coincide with the central radio component. A* 19ᵐ *companion galaxy appears to lie in the region of the Np radio component.*

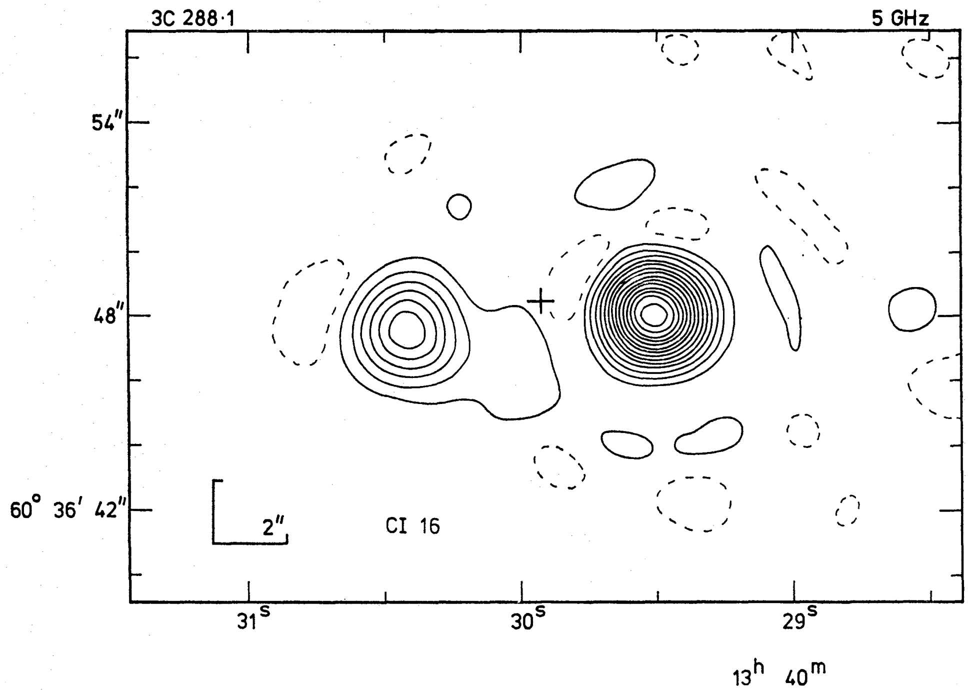

Fig. 2. 3C 288.1. *The position (AK, MTC) of the* 18m *QSO is marked.*

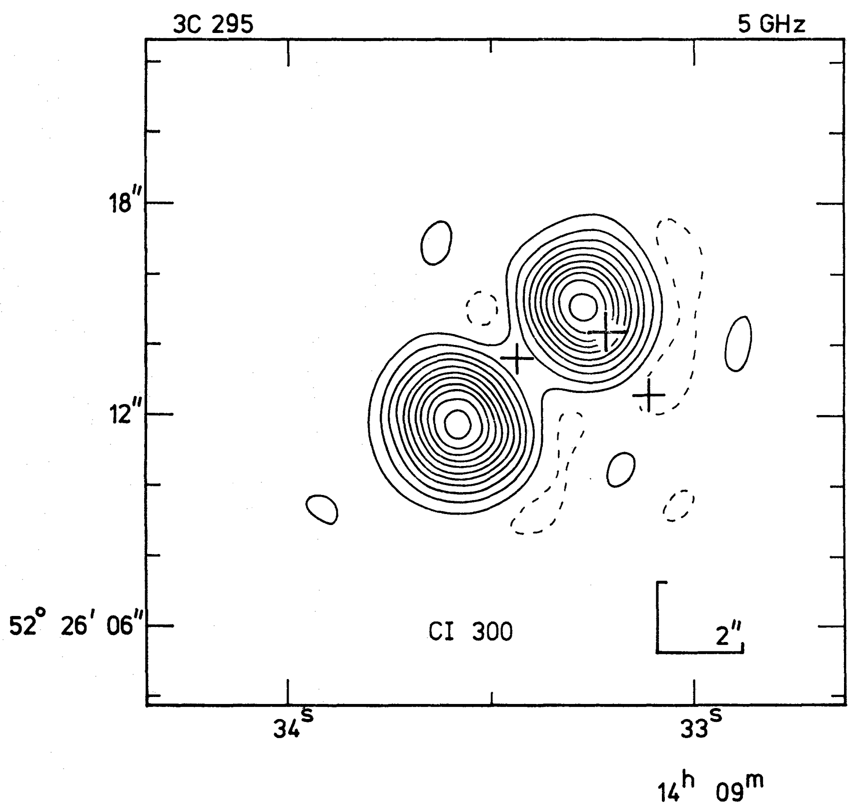

Fig. 2. 3C 295. *The positions (G) of the* 21m *galaxy at the centre of the radio source and its two nearest neighbours are marked.*

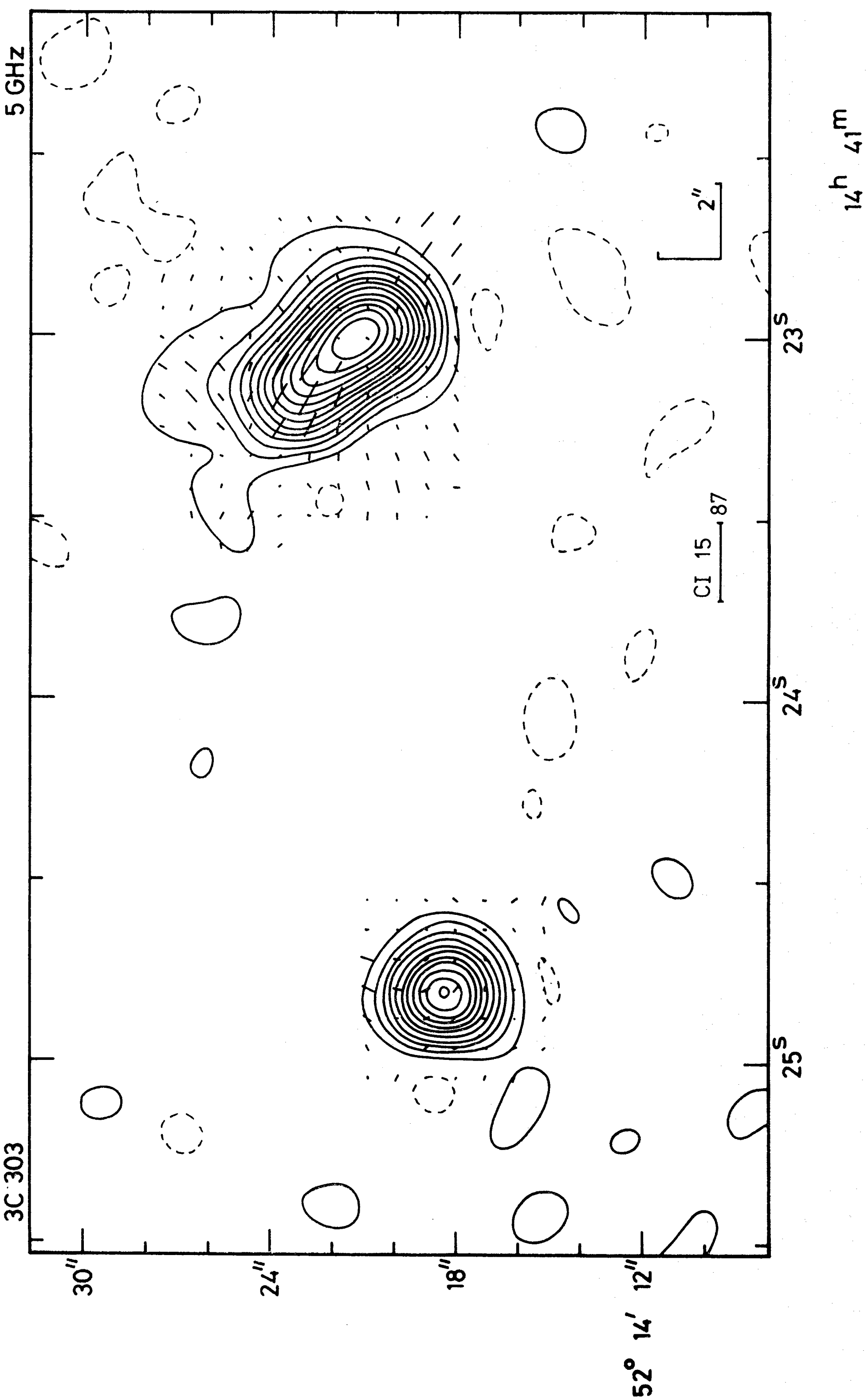

FIG. 2. 3C 303. *The identification is in doubt; see text.*

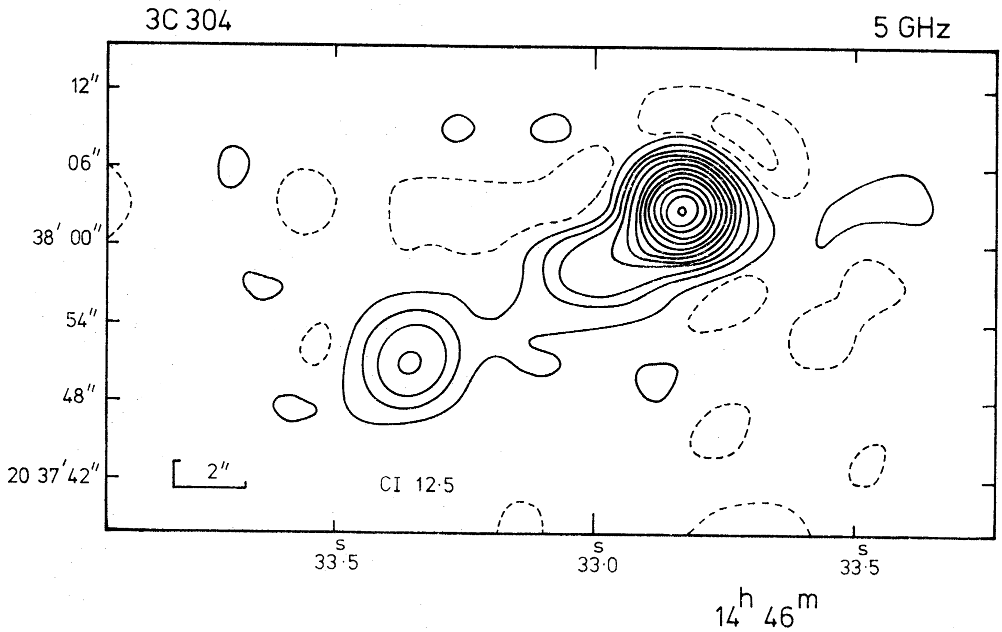

FIG. 2. 3*C* 304. *The position of an* 18m *cD galaxy* (*Olsen* 1970) *is marked. The source, also catalogued as* 4*C* 20.34, *is not included in the revised* 3*C catalogue* (S_{178} = 5·4 *fu*).

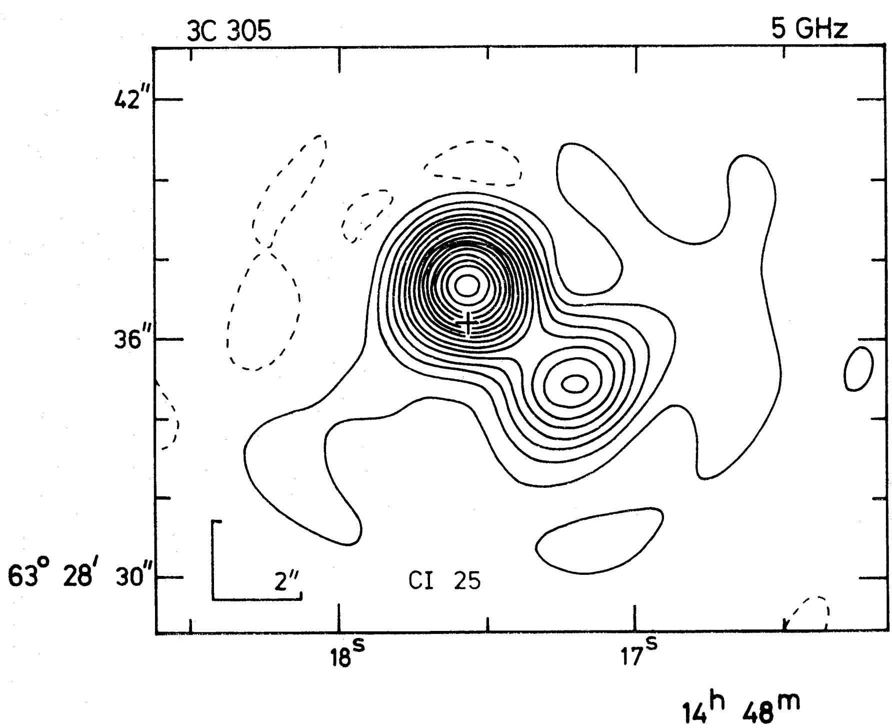

FIG. 2. 3*C* 305. *The position* (*V*) *of the nucleus of the peculiar galaxy discussed by Sandage* (1966) *is marked. The radio source is apparently embedded in the optical galaxy. There is a low brightness region surrounding the compact components.*

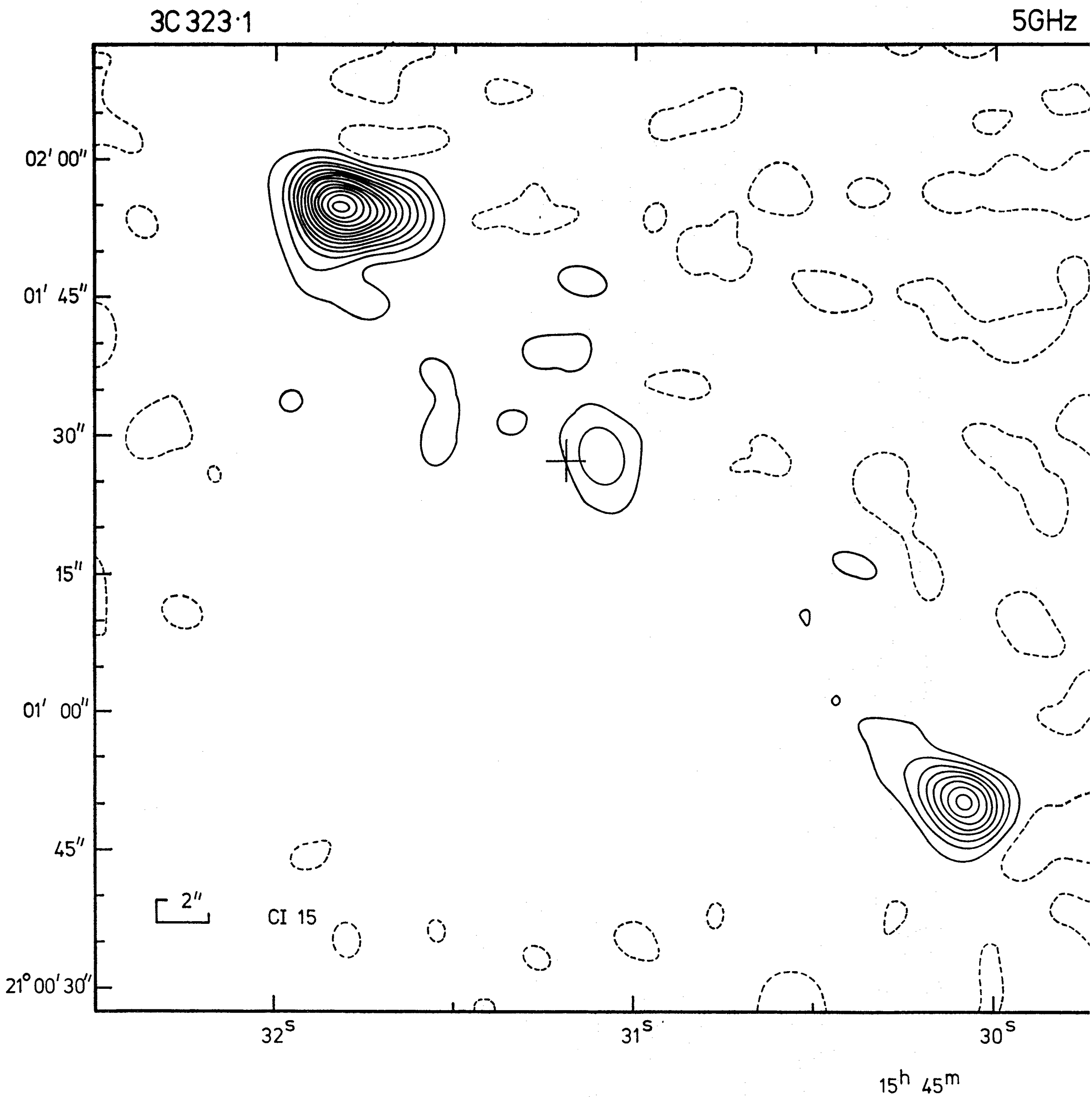

FIG. 2. 3C 323.1. *The position* (*Véron & Véron* 1973) *of the* 17m *QSO is marked. There is a faint bridge of emission joining the outer components. The redshift is* 0·264, *close to that of a nearby cluster of galaxies* (*Oemler* et al. 1972).

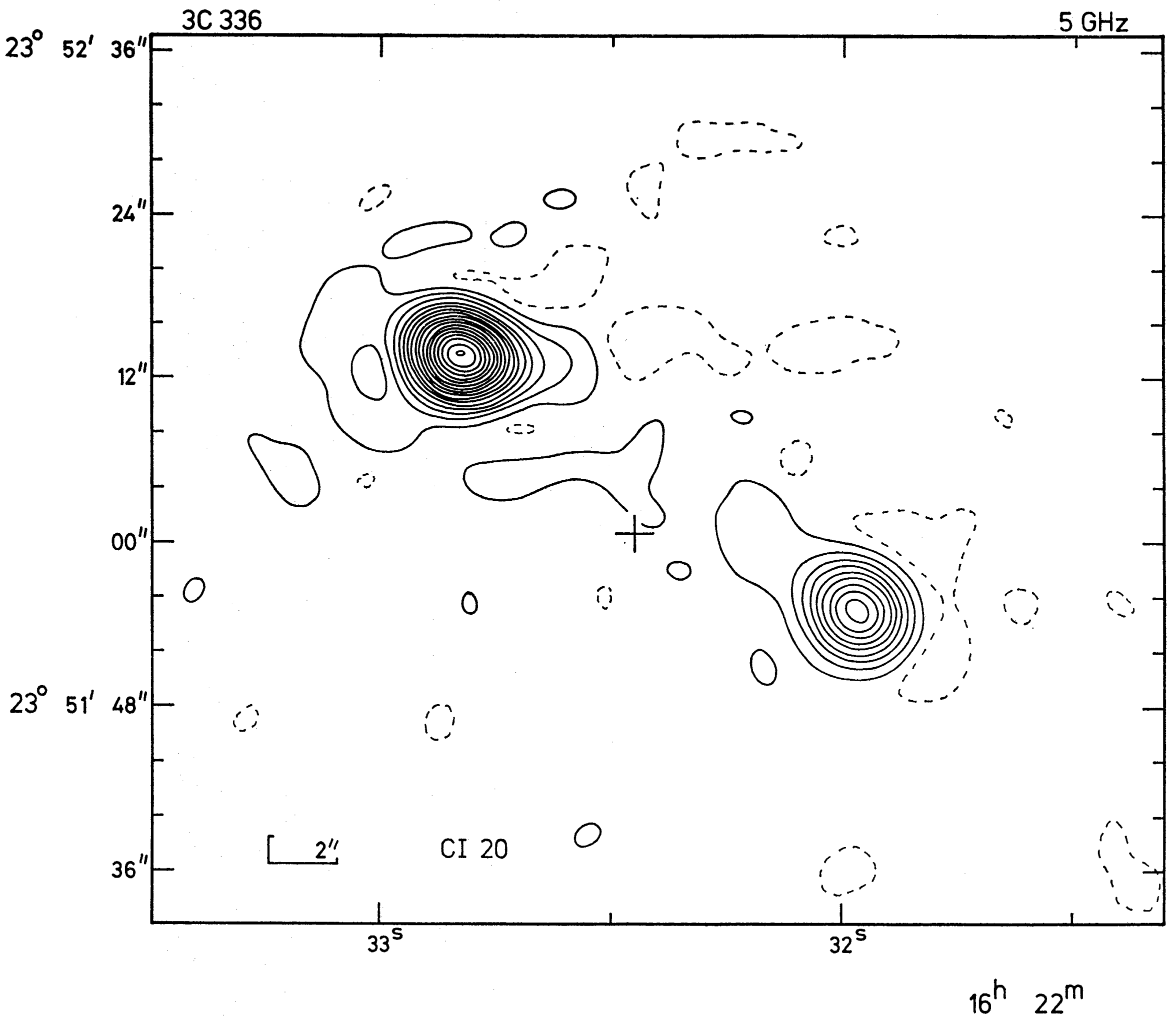

FIG. 2. 3*C* 336. *The position (SVW) of the* 17m *QSO is marked.*

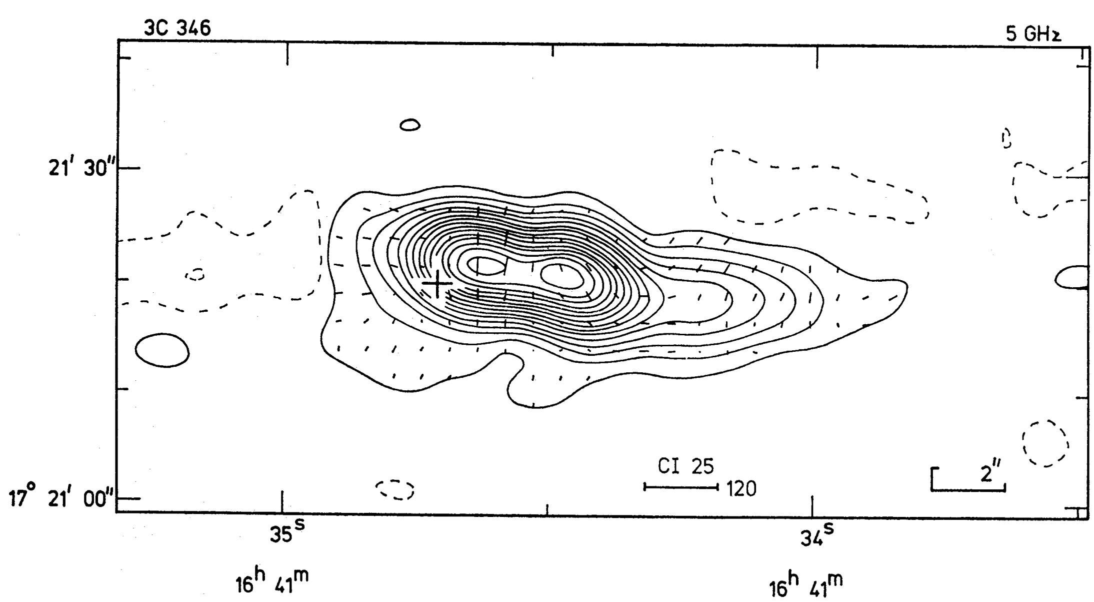

FIG. 2. 3*C* 346. *The position (V) of the* 16m *galaxy is marked.*

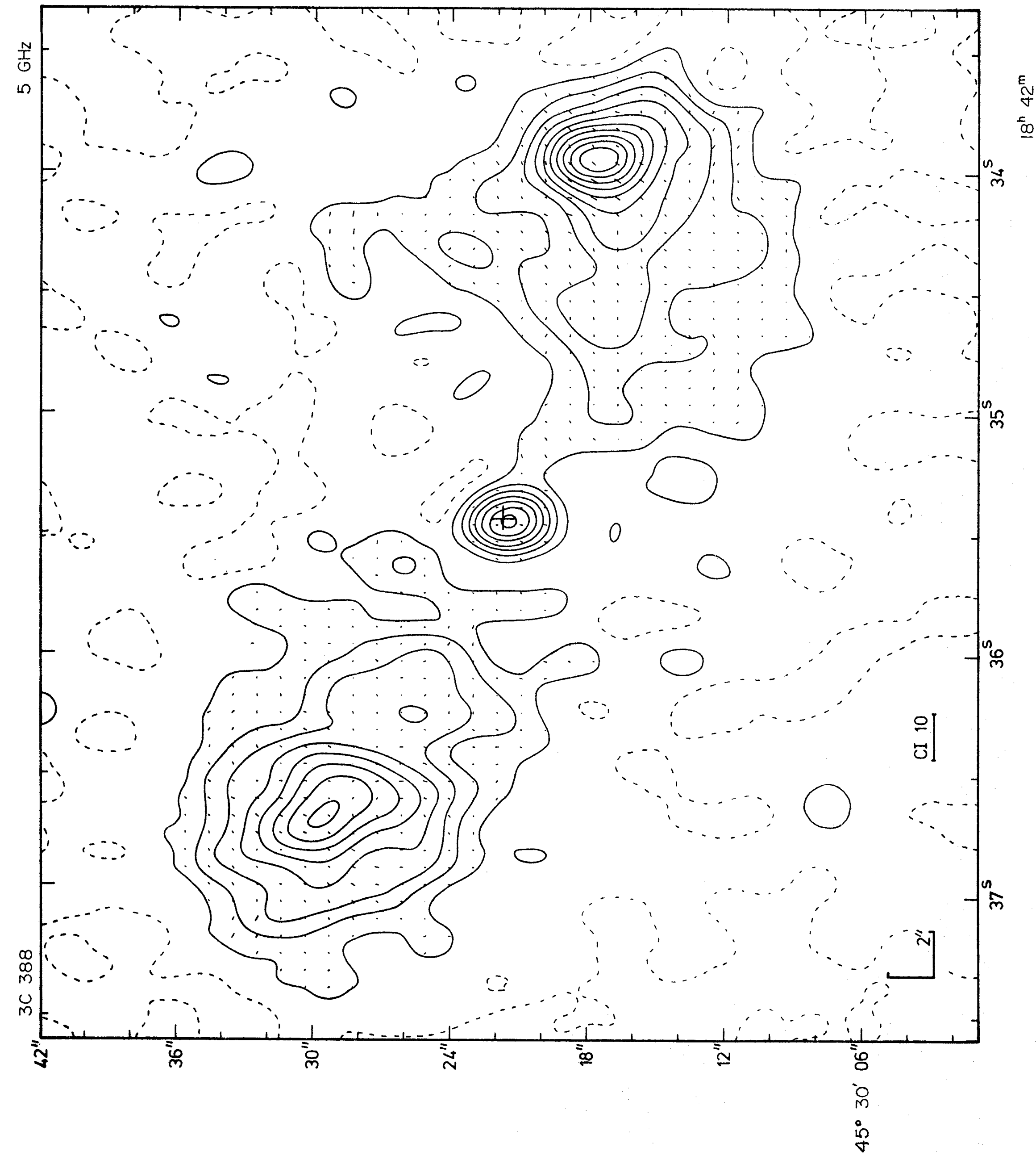

Fig. 2. *3C 388. This map is not compressed in declination. The position (G) of the nucleus of the* 15^{m} *cD3*

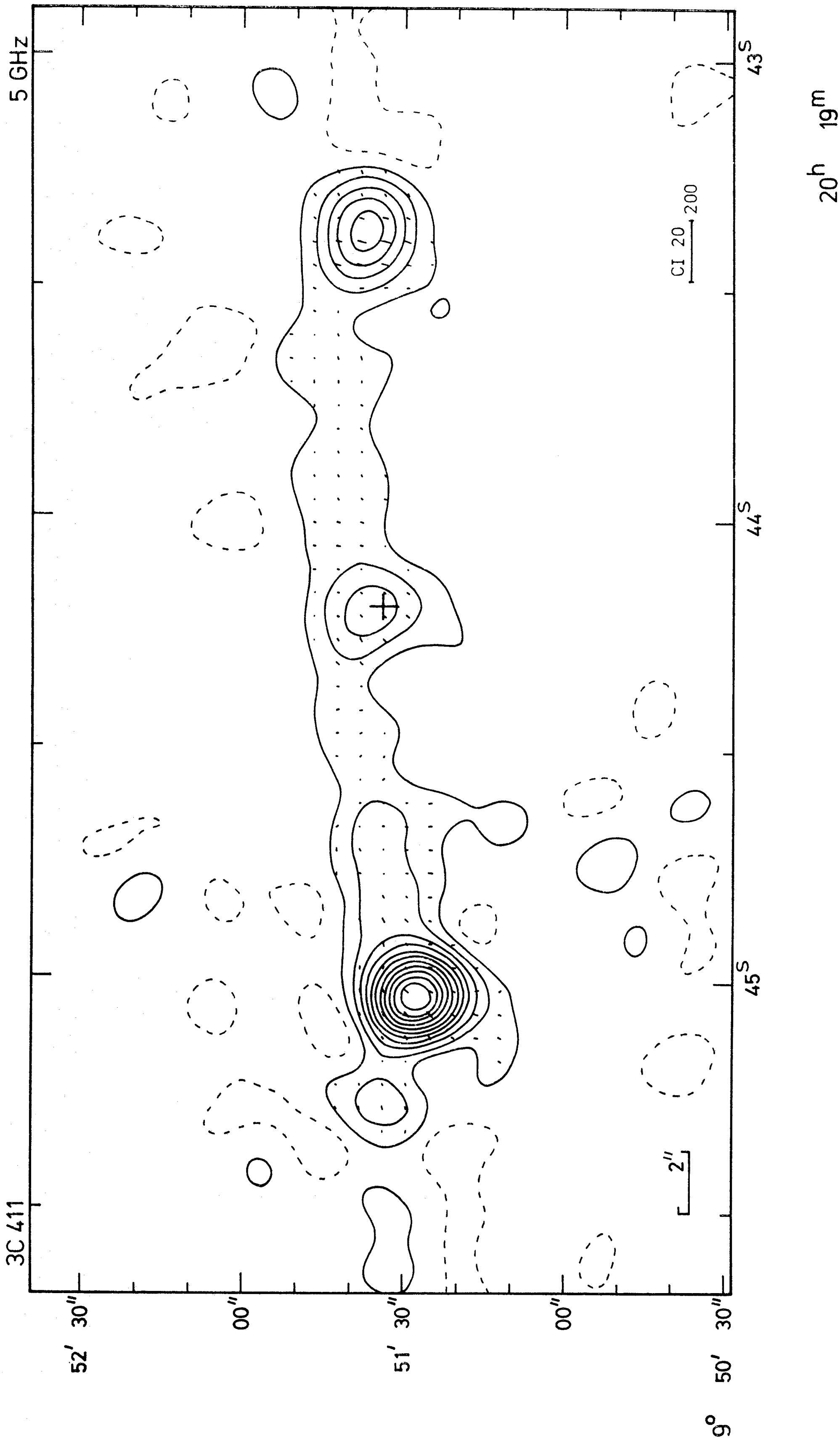

FIG. 2. 3C 411. *This source is discussed in more detail by Spinrad* et al. (1974), *who also give the position of the* 20^{m} *N galaxy marked.*

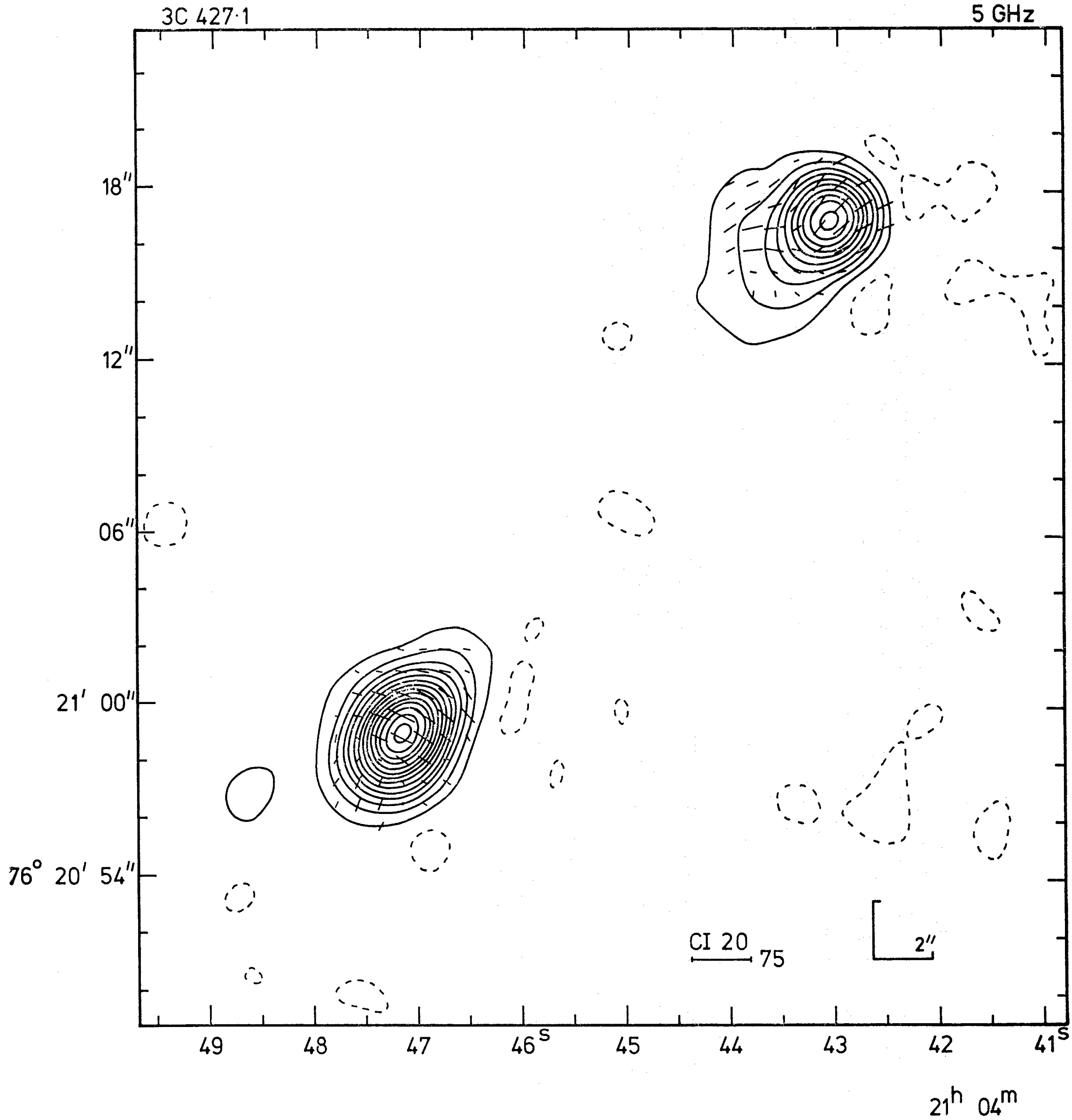

FIG. 2. 3C 427.1. *There is no optical identification.*

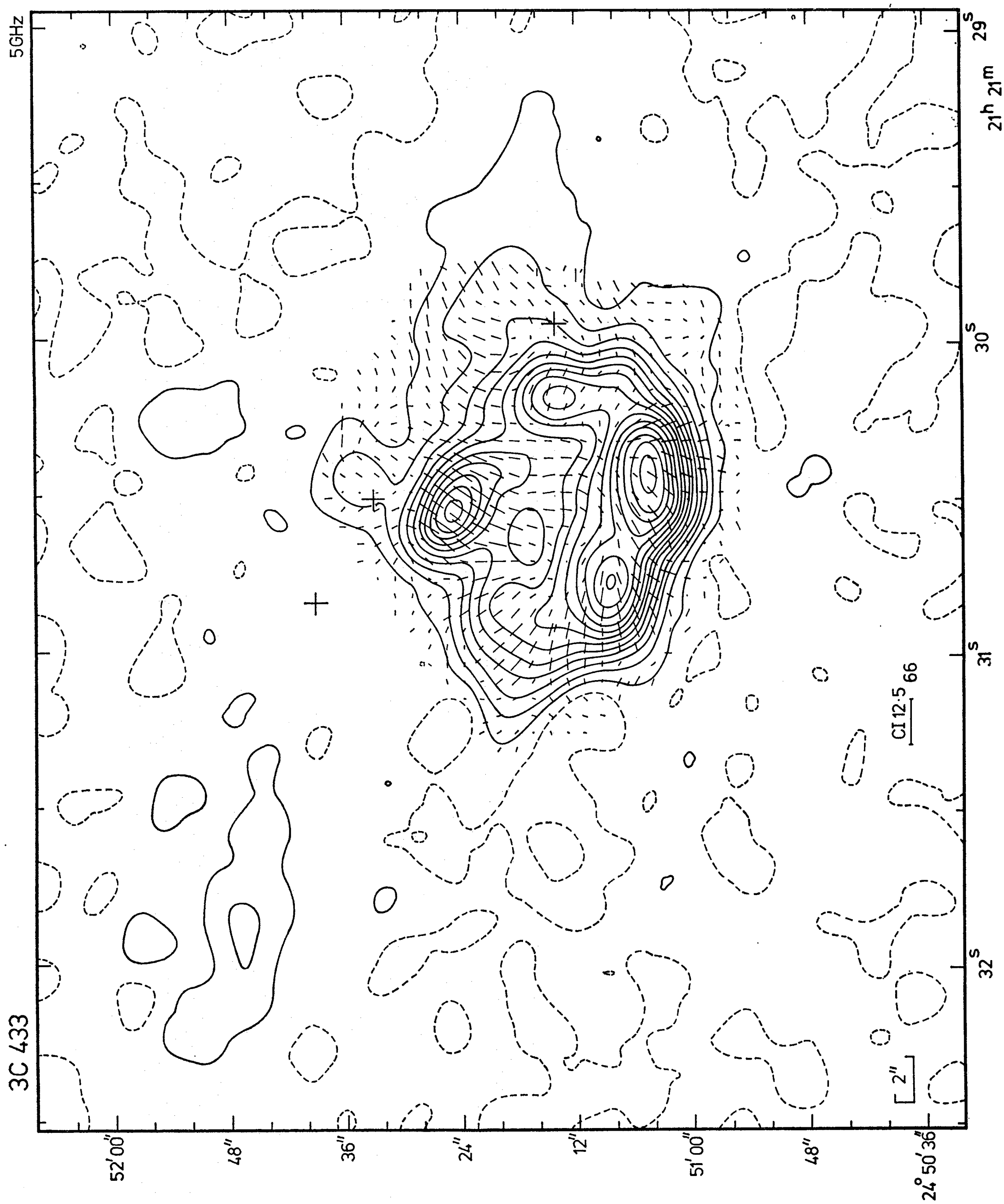

FIG. 2. 3C 433. *The total angular extent of the emission to the NE of the source is over 70″. The two northern crosses are at the positions of two galaxies (G); the third cross marks a fainter galaxy.*

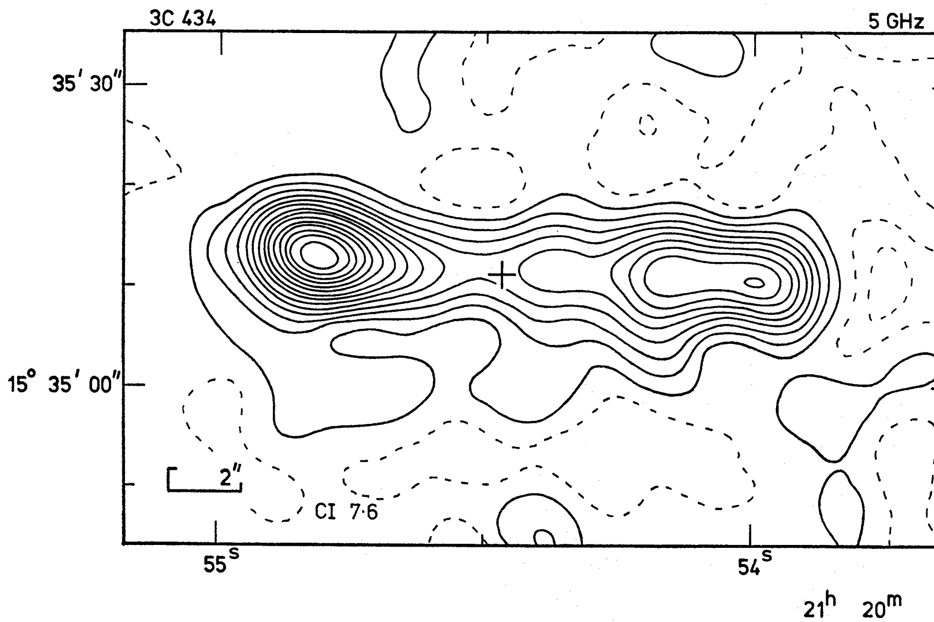

FIG. 2. 3*C* 434. *The position* (*GL*) *of a* 21^{m} *N galaxy* (*Spinrad & Smith* 1974) *is shown. Two possible redshifts suggested by Spinrad & Smith are used in the table.*

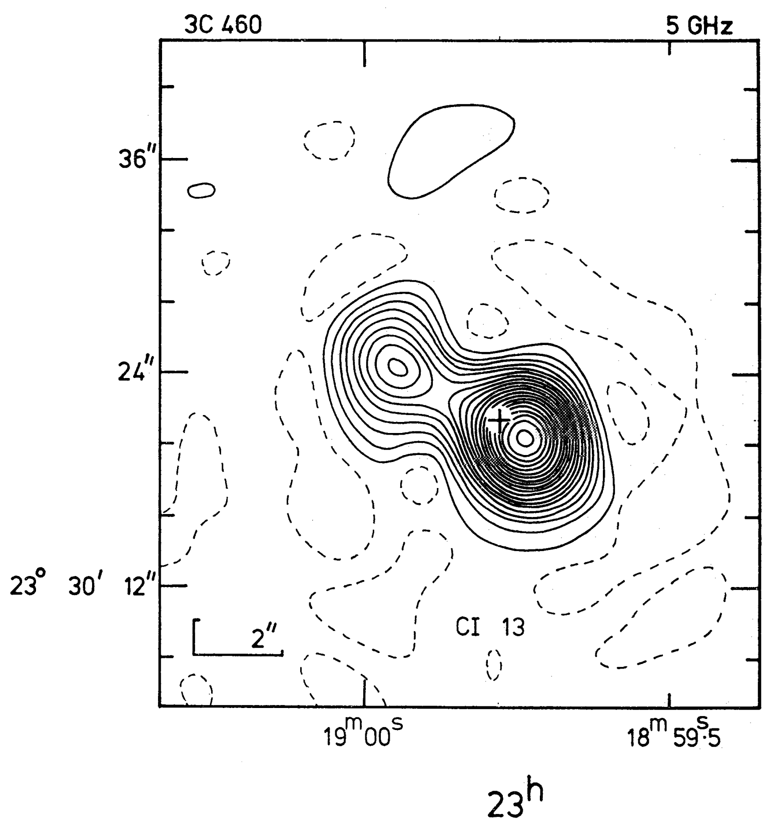

FIG. 2. 3*C* 460. *The position* (*Wlérick* et al. 1971) *of an* 18^{m} *E5 galaxy is marked.*

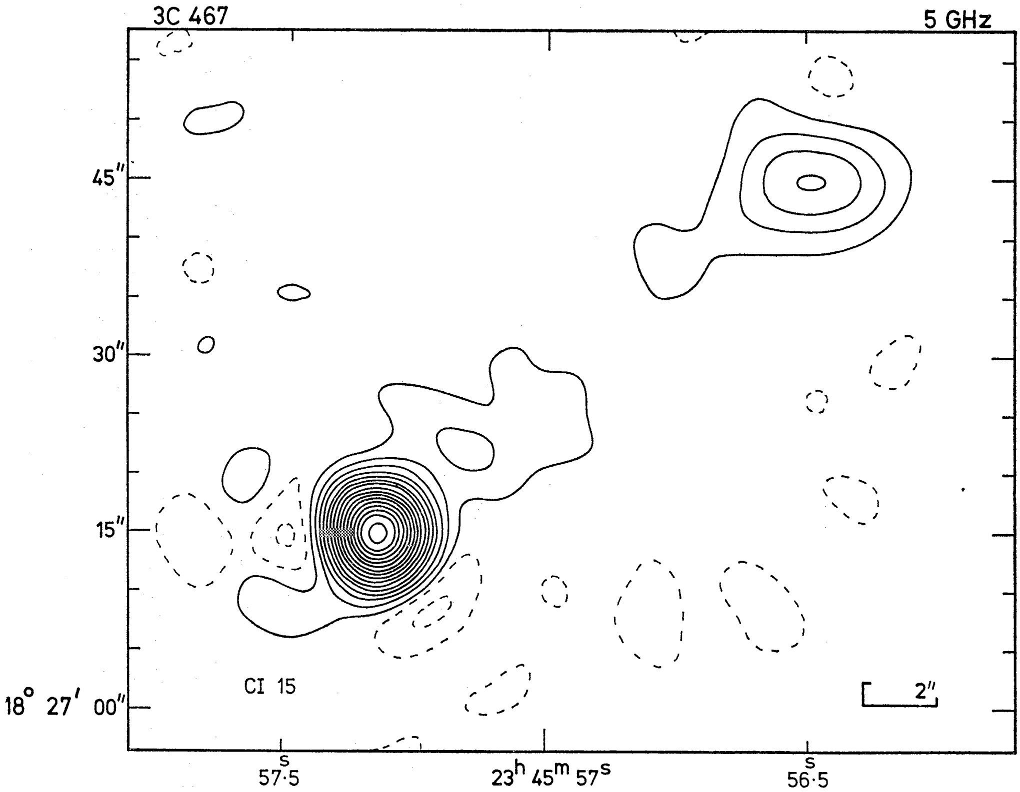

FIG. 2. 3C 467. *The identification is a* 20^m *N galaxy* (*Spinrad & Smith* 1974) *whose position is not well known. The source, also catalogued as* 4C 18.71, *is not in the revised* 3C *catalogue* (S_{178} = 7·6 *fu*).

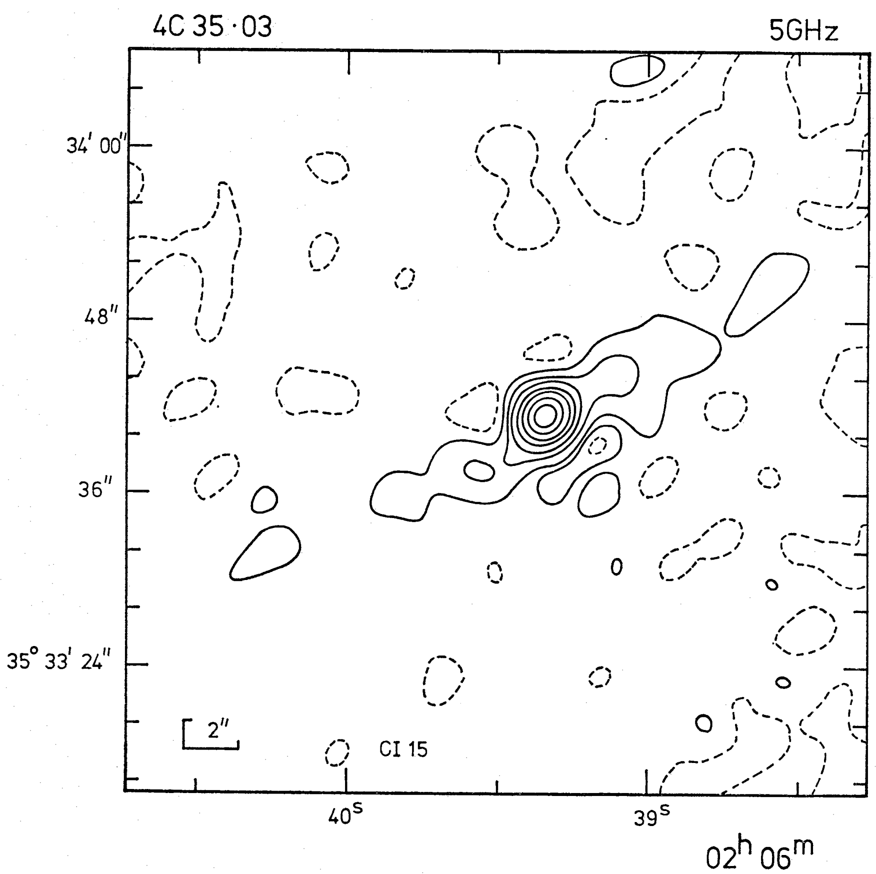

FIG. 2. 4C 35.03. *The* 14^m *galaxy* (*Olsen* 1970), *catalogued as VV* 6-5-88 *and number* 191 *in Zwicky's fifth list of compact galaxies is coincident with the compact radio component.*

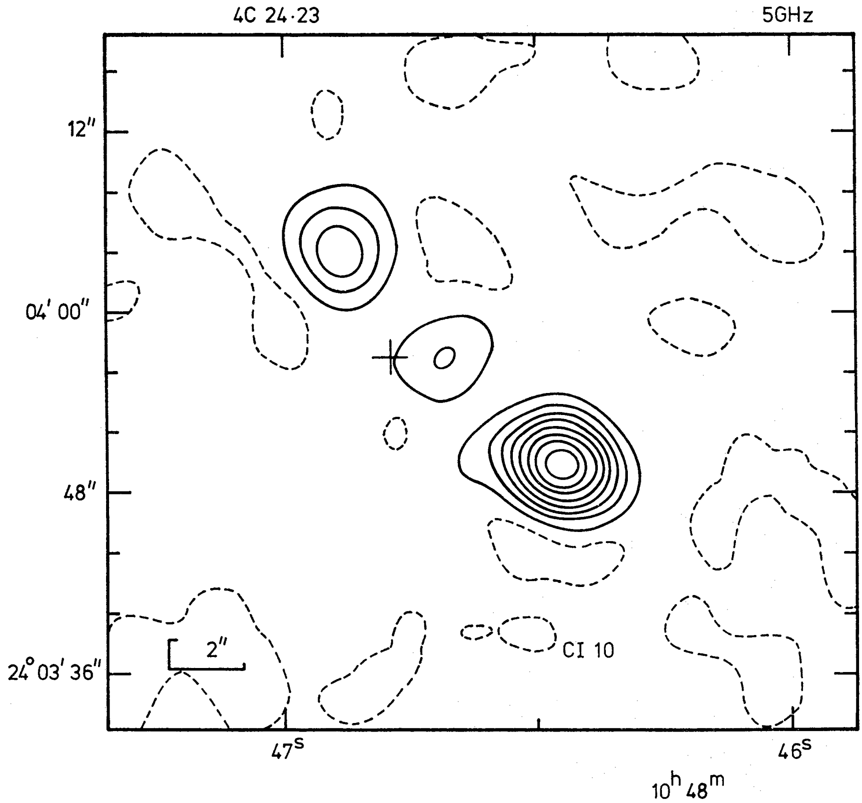

FIG. 2. 4*C* 24.23. *The position* (*Hazard & Argue, private communication*) *of the* 18m·5 *QSO is marked.*

structure must be considered carefully. The angular scale of each map is shown by the ' L ' shape in the corner, the length of whose arms is shown. The intensity scale for each map is shown by the contour interval (the flux density of an unresolved source which would produce a change of one contour on the map, indicated by ' CI '), and the scale of linear polarization is indicated by the length of the bar. All units are mfu. Further details are given in the captions; in particular, measurements of optical positions are referred to as follows:

AK	Argue & Kenworthy (1972)
BCGP	Barbieri *et al.* (1972)
G	Griffin (1963)
GL	Gunn & Longair (1975)
KSK	Kristian, Sandage & Katem (1974)
MTC	Murray, Tucker & Clements (1971)
SVW	Sandage, Véron & Wyndham (1965)
L	Longair (1965)
V	Véron (1966, 1968)
WWD	Wills, Wills & Douglas (1973)

Reference is not necessarily made here to the original identification or redshift determination.

No maps are shown for six sources: 3C 67, 3C 236, 3C 268.3, 3C 277.1, 3C 454.1 and 4C 25.03. These all have angular sizes comparable with the beam of the telescope.

The data for each source are given in Table I. The sources are divided into components for the purposes of this table. The division is in many cases entirely natural, when the map shows several more or less unresolved features. In some cases it also appears reasonable to describe sources in terms of unresolved and resolved components, but the division must then be to some extent arbitrary, and the tables must of course be read in conjunction with the maps. The details are as follows:

(1), (18) Source number from the 3C or 4C catalogues (Edge *et al.* 1959; Bennett 1962; Pilkington & Scott 1965).

(2), (3) 1950·0 coordinates of the peaks of emission, with estimated errors. Components without a well-defined peak are given only an approximate position.

(4) The position angle of each component. Errors in these angles are typically 5° to 10°.

(5), (6) The angular extent of each component parallel and perpendicular to the position angle given in (4). A gaussian brightness distribution is assumed when the component is barely resolved.

(7) The flux density of each component at 5 GHz, with estimated error. Relatively large errors are given if the source is divided into several parts, with a consequent uncertainty in the division, or if the surface brightness is low.

(8) The percentage polarization, with estimated error. Upper limits are given if the polarized flux is less than 20 mfu and the total flux of the component is more than 40 mfu.

(9) The position angle of the E vector of the polarized flux. For complex sources (e.g. 3C 123) reference should be made to the maps.

(10) The total angular size of the source. This is usually the separation of the outer peaks of a multiple source.

(11) Position angle of the line joining the outer peaks.

(12) Redshift.

(13) Distance. For galaxies without measured redshift an absolute V magnitude of $-23{\cdot}2$ has been assumed. In this and succeeding columns an Einstein–de Sitter model with $H = 50\ \mathrm{km\ s^{-1}\ Mpc^{-1}}$ has been assumed.

(14) The total linear size of the source, corresponding to the angular size in column 10.

(15) An estimate of the minimum energy in the component, assuming emission by the synchrotron process from electrons. Each component is assumed to be cylindrical in symmetry about the longest axis, and this axis is assumed to be normal to the line of sight. The formula used is that given on page 394 of Branson *et al.* (1971); for most sources the mean overall spectral index has been used. A spectral index (defined by $S \propto \nu^{-\alpha}$) of zero has been assumed for central components not previously observed and with no information on their spectral indices, since, in cases where the spectrum of this type of source is known, $\alpha \approx 0$.

(16) The value of the magnetic field corresponding to the minimum energy.

(17) The half-life for an electron radiating near 5 GHz in this field.

TABLE I

Source 3C	R.A. h	m	s	± s	Dec °	'	"	± "	p.a. °	Component ω max "	ω min "	Flux density mfu	±
6.1	00	13	32.73	0.04	78	59	59.5	0.1	105	1.3	< 0.9	420	40
			34.40	0.15	79	00	10.0	0.4				20	10
			36.62	0.04	79	00	22.8	0.1	0	< 0.9	< 0.9	540	50
9	00	17	49.71	0.02	15	24	19.3	1.5	177	8	1.6	110	10
			50.13	0.02			11.2	1.0	140	10	< 3.2	370	50
47	01	33	38.95	0.01	20	41	38.7	0.5	98	3.2	1.8	400	50
			39.5				37		98	10	6	160	50
			40.42	0.01	20	42	10.6	0.5	0	< 4	< 1	80	10
			41.79	0.02			34.7	0.8	112	5.0	3.7	190	40
			41.5				30		117	15	11	230	40
67	02	21	18.05	0.01	27	36	37.8	0.3				1000	50
68.2	02	31	24.38	0.01	31	21	21.1	0.2	156	2.0	< 1.3	120	10
			25.12	0.01			01.0	0.2	0	< 1.8	< 1	80	10
69	02	34	17.31	0.02	58	58	29.2	0.1	0	< 1.1	< 1	90	30
			16.7				29		41	11	5	380	40
			18.58	0.03		58	51.9	0.2	0	< 1.3	< 1	30	10
			19.53	0.02		59	13.6	0.1	0	< 1.1	< 1	200	30
			19.3				07		13	8	2.5	350	30
86A	03	23	29.09	0.03	55	10	01.9	0.3	168	6	3.5	1700	200
			32.20	0.02			04.0	0.2	0	< 1	< 1	500	100
			31.6				00		55	9	4	900	200
86B	03	23	55.31	0.03	55	12	06.3	0.3	0	< 1.5	< 1.5	190	50
			55.86	0.03			00.1	0.3	0	< 2	< 2	100	30
123	04	33	54.8		29	34	27		90	12	8	5600	400
			55.79	0.01			09.7	0.3	70	1.2	< 1.8	6600	500
			55.5				04		22	15	8.5	4800	500
153	06	05	44.10	0.1	48	04	46.4	0.5	45	3.7	< 1	730	50
			44.63	0.02			50.2	0.2	0	< 1.2	< 1	780	80
171	06	51	10.43	0.02	54	12	49.0	0.2	0	< 1.1	< 0.9	430	40
			11.42	0.02			47.3	0.2	12	1.7	< 0.9	350	40
181	07	25	20.11	0.01	14	43	48.1	0.4	173	4.1	2.8	280	20
			20.47	0.01			45.6	0.4	0	< 4	< 1	520	50

TABLE I—*continued*

Polarization			θ	p.a.	z	Dis-tance (Mpc)	Total size (kpc)	U_{min} (10^{56} erg)	B_{eq} (10^{-5} G)	5GHz Synch. lifetime (10^4 yr)	Source
%	±	p.a. o	"	o							3C
7	1	0	26.0	26		2800	206	< 240	> 15	< 13	6.1
-											
5	1	85						< 240	> 17	< 11	
< 20			10.0	143	2.012	5085	82	5300	15	13	9
14	3	29						< 6000	> 10	< 20	
21	2	33	69	35	0.425	1950	450	320	7	41	47
47	10	111									
-								920	1.9	290	
< 20								< 15	> 3	< 160	
< 20								470	3.3	130	
-								2100	1.4	460	
< 2			2.0	176	0.301	1500	11				67
20	5	105	22.3	155							68.2
< 20											
15	5	143	47.7	21							69
-											
-											
10	3	63									
< 40											
20	5	91	26.7	86							86A
8	1	88									
< 20											
< 12			6.6	140							86B
< 20											
see notes			23.7	138		2000	160	< 2500	> 7	< 39	123
2.5	0.1	170						< 800	> 17	< 11	
see notes								7500	3.2	130	
8	1	122	6.5	54	0.2771	1380	34	< 100	> 8	< 30	153
8	1	44						< 66	> 12	< 18	
< 4			8.9	102	0.2387	1220	42	< 30	> 12	< 18	171
9	2	125						< 32	> 10	< 24	
< 7			5.9	114	1.382	4220	51	2200	7	41	181
< 4								< 1300	> 15	< 13	

TABLE I—*continued*

Source 3C	R.A. h	m	s	± s	Dec °	'	"	± "	p.a. °	ω	Component max "	ω	min "	Flux density mfu	±
194	08	06	37.74	0.01	42	37	02.4	0.2	63		1.4	<	1.3	410	40
			38.19	0.01		36	49.1	0.2	173		1.7	<	0.9	270	30
196	08	09	59.28	0.02	48	22	04.9	0.2	90		1.2	<	1.3	2500	200
			59.50	0.02			09.7	0.2	128		1.2	<	1.2	1600	200
			59.8				08		120		2	<	1	400	200
204	08	33	15.37	0.03	65	24	05.0	0.2	63		1.4	<	1	50	10
			16.01	0.03			06.2	0.2	40		1.5	<	1	100	20
	preceding bridge								85		5	<	1	40	20
			18.07	0.03			04.1	0.2	0	<	1	<	1	40	10
			20.97	0.03			03.1	0.2	157		2.0	<	1	130	20
	following bridge								79		5	<	1	40	20
205	08	35	09.80	0.01	58	04	42.9	0.1	145		2.0	<	1	500	50
			10.02	0.06			51.5	0.6	0	<	1.1	<	1	30	10
			10.30	0.01			58.4	0.2	0		1.6	<	1	190	20
207	08	38	01.46	0.02	13	23	06.6	0.6	0	<	5	<	1	200	20
			01.74	0.02			05.3	0.6	0	<	5	<	1	510	30
			02.1				05		0		9		5	530	50
215	09	03	43.3	0.2	16	58	33.0	3	90		8		8	160	70
			44.11	0.02			16.0	1	0	<	6	<	2	20	10
			44.73	0.05			12.8	.2	0		12		5	150	50
236	10	03	05.39	0.01	35	08	48.0	0.2						1480	30
239	10	08	38.29	0.02	46	43	06.8	0.2	45		1.5	<	1.1	70	10
			39.33	0.01			09.8	0.1	0	<	1.2	<	1	260	30
249.1	11	00	22.81	0.04	77	15	11.4	0.1	116		1.3		1.0	250	40
			23.8				11		0		3.5		2	120	40
			27.44	0.06			08.5	0.2	0	<	1.1	<	1	110	20
			29.72	0.04			08.3	0.1	80		1.3	<	1	160	30
			28.6				08		95		2	<	1	50	30
254	11	11	52.29	0.01	40	53	44.2	0.2	0	<	1.4	<	1.4	400	50
			53.41	0.01			40.6	0.2	55		1.6	<	1.3	430	50
263	11	37	04.99	0.03	66	04	37.2	0.2	28		1.4		1.3	60	20
			04.5				38		95		2.7		1.8	90	20
			09.30	0.02			27.05	0.1	0	<	1	<	1	130	20
			11.78	0.02			21.0	0.1	0	<	1	<	1	750	70
268.3	12	03	54.08	0.02	64	30	18.45	0.1						1250	30

TABLE I—*continued*

Polarization %	±	p.a. °	θ "	p.a. °	z	Distance (Mpc)	Total size (kpc)	U_{min} (10^{56} erg)	B_{eq} (10^{-5} G)	5GHz Synch. lifetime (10^{4} yr)	Source 3C
11	2	77	14.2	151		2300	100	< 230	> 11	< 21	194
< 10								< 140	> 11	< 21	
2.5	0.3	128	5.0	26	0.871	3230	41	< 1200	> 22	< 7	196
7	1	130						< 900	> 20	< 8	
23	3	47						< 320	> 16	< 12	
< 36			31.1	95	1.112	3740	270	< 250	> 11	< 21	204
30	6	140						< 390	> 14	< 15	
-								< 370	> 7	< 34	
< 36								< 21	> 4	< 95	
< 16								< 460	> 14	< 15	
-								< 370	> 7	< 34	
14	2	72	15.9	14	1.534	4460	135	< 1200	> 21	< 8	205
-								< 25	> 4	< 80	
< 10								< 580	> 18	< 10	
< 10			8.4	100	0.684	2750	66	< 270	> 6	< 49	207
6	1	11						< 50	> 7	< 38	
< 10								2000	3.1	140	
-			28.5	133	0.411	1900	185	1100	2.0	270	215
-								< 19	> 1.6	< 400	
< 40								880	2.1	250	
< 2			0.78	120	0.0988	550	1.9				236
30	10	101	11.2	75		2300	80	< 300	> 14	< 15	239
< 7								< 120	> 12	< 15	
< 8			23.0	98	0.311	1520	130	38	8.7	30	249.1
< 40								61	3.9	99	
20	5	0						< 6	> 4	< 90	
< 11								< 27	> 8	< 30	
< 40								< 16	> 5	< 60	
9	3	120	13.2	105	0.734	2890	110	< 540	> 13	< 15	254
< 4								< 570	> 14	< 15	
< 35			44.2	111	0.652	2660	345	87	5.9	53	263
< 40								190	4.6	77	
< 14								< 22	> 5	< 70	
< 2								< 190	> 114	< 14	
< 2			1.28	157		1740	7.6				268.3

TABLE I—*continued*

Source	R.A.			±	Dec			±	p.a.	Component		Flux density	
3C	h	m	s	s	°	′	″	″	°	ω max ″	ω min ″	mfu	±
268.4	12	06	41.83	0.01	43	55	58.2	0.1	0	< 1.4	< 1.2	570	40
			42.10	0.05		56	02.3	0.7				50	20
			42.42	0.02			06.0	0.3	40	1.8	< 1.2	110	30
277.1	12	50	15.19	0.01	56	50	36.5	0.1				840	20
277.3	12	51	45.71	0.02	27	54	07.5	0.4	151	2.4	2.2	90	30
			45.7			53	58		90	19	12	540	70
			46.29	0.02			48.8	0.5	25	2.4	< 1.5	20	10
			46.28	0.02			35.9	0.5	69	11	10	660	80
280	12	54	40.78	0.01	47	36	32.2	0.1	148	1.6	< 1.1	1480	150
			42.05	0.02			32.0	0.3	0	< 1.2	< 1	400	40
288	13	36	38.3		39	06	27.5		106	10	3.5	520	60
			38.59	0.03			22.2	0.5				30	20
			38.79	0.03			17.5	0.5	138	3.5	2.8	180	50
			38.4				18		90	11	3	310	50
288.1	13	40	29.51	0.01	60	36	48.0	0.1	0	< 1	< 1	270	30
			30.42	0.02			47.5	0.2	56	1.3	1.3	130	20
295	14	09	33.27	0.01	52	26	15.1	0.1	0	0.7	0.7	2900	300
			33.58	0.01			11.7	0.1	0	1.0	1.0	3600	300
303	14	41	23.00	0.05	52	14	21.4	0.6	34	4.4	1.3	510	40
			24.82	0.01			18.2	0.2	0	< 1.2	< 1.1	200	20
304	14	46	32.83	0.02	20	38	03.0	0.6	0	< 2.5	< 1	160	20
			33.0			38	00		149	13	< 2.5	100	20
			33.36	0.02		37	51.2	0.6	0	< 2.5	< 1	60	10
305	14	48	17.22	0.02	63	28	34.9	0.2	128	1.9	1.1	290	40
			16.9				36		128	2.9	2.4	80	40
			17.57	0.02			37.3	0.2	0	1.4	1.3	570	60
323.1	15	45	30.08	0.01	21	00	50.3	0.3	27	3.2	< 2.2	160	20
			31.09	0.02		01	27.8	0.4	5	3.6	< 1.1	50	10
			31.82	0.02			54.7	0.3	176	3.5	3.0	440	40
336	16	22	31.97	0.01	23	51	55.1	0.4	30	2.3	< 1.9	240	30
			32.2			52	00		30	3.7	< 1.9	30	10
			32.83	0.01		52	13.5	0.4	78	1.8	< 2.3	490	40

TABLE I—*continued*

Polarization %	Polarization ±	Polarization p.a. °	θ ″	p.a. °	z	Distance (Mpc)	Total size (kpc)	U_{min} (10^{56} erg)	B_{eq} (10^{-5} G)	5GHz Synch. lifetime (10^4 yr)	Source 3C
14	2	35	10.2	39	1.40	4250	87	< 1200	> 21	< 8	268.4
< 21											
< 15								< 530	> 12	< 18	
2			1.26	132	0.321	1560	7.2				277.1
< 30			22.4	169	0.0857	480	48	2.7	3.2	130	277.3
-								78	1.1	660	
-								< 0.3	> 2	< 340	
< 30								58	1.6	380	
12	1	40	12.9	91		2300	95	< 420	> 16	< 12	280
9	2	115						< 150	> 13	< 16	
< 20			11.5	151		690	34	90	3.7	110	288
-								< 0.5	> 3	150	
< 20								26	4.1	92	
30	15	105						64	3.3	130	
< 7			6.7	94	0.961	3430	57	< 400	> 17	< 11	288.1
< 15								370	11	21	
< 0.5			4.3	140	0.4614	2070	29	190	28	5.1	295
< 0.5								330	22	7.4	
50	10	59	16.9	100							303
< 9											
			14	149	0.254	1280	69	< 34	> 7	< 40	304
								< 110	> 2	< 220	
								< 19	> 5	< 70	
< 9			3.4	44	0.0416	240	3.8	0.8	11	21	305
-								0.9	4.2	88	
< 4								1.2	13	16	
< 13			68.2	22	0.264	1330	350	< 63	> 4	< 110	323.1
< 40								< 6	> 2	< 250	
< 7								150	4.1	92	
< 8			21.7	33	0.927	3360	180	< 750	> 8	< 32	336
-								< 280	> 4	< 95	
< 5								< 1200	> 10	< 25	

TABLE I—*continued*

Source	R.A.			±	Dec			±	p.a.	Component		Flux density	
3C/4C	h	m	s	s	°	'	"	"	°	ω max "	ω min "	mfu	±
346	16	41	34.48	0.02	17	21	20.8	0.6	74	5.4	< 3	1280	60
			34.63	0.02			21.6	0.6					
			34.2				18		90	3.5	< 3	300	50
388	18	42	33.94	0.02	45	30	17.7	0.2	3	2.1	1.3	110	70
			34.2				17		96	14	12	790	70
			35.45	0.02			21.6	0.2	0	< 1.3	< 1	100	30
			36.66	0.02			29.4	0.2	51	4.0	2.2	130	60
			36.4				26		51	14	10	790	60
411	20	19	43.375	0.01	9	51	37.5	1.0	25	3.5	< 5	160	80
			44.20	0.02			33.8	1.5	0	< 5.3	< 0.9	30	10
	bridge								115	26	8	570	150
			45.04	0.01			27.7	0.6	0	7	< 0.9	250	100
427.1	21	04	43.07	0.03	76	21	17.0	0.1	136	5.7	2.3	430	30
			47.15	0.03		20	59.0	0.1	146	2.9	1.5	610	70
433	21	21	30.5		24	51	14		0	28	16	3900	400
			32				48		80	30	13	500	100
434	21	20	54.1		15	35	11		90	6	< 5	270	30
			54.8	0.1			13.5	1	72	4	< 4	230	30
454.1	22	48	58.87	0.02	71	13	23.75	0.1				310	10
460	23	18	59.74	0.01	23	30	20.3	0.3	3	2.8	< 1	320	40
			59.95	0.02			24.3	0.4	0	< 2.0	< 1.4	130	20
467	23	45	56.49	0.03	18	27	44.8	0.4	66	2.1	< 2.9	120	20
			57.31	0.02			15.0	0.4	0	< 3.5	< 1	310	30
			57.0				25		146	7.5	4.3	70	20
25.03	01	00	07.92	0.01	25	36	09.0	0.3	0	< 2.0	< 1	310	30
35.03	02	06	39.34	0.02	35	33	41.4	0.4	0	< 1.6	< 1	100	20
			39.4				40		138	40	12	800	150
24.23	10	48	46.45	0.01	24	03	49.8	0.3	60	1.6	< 2.1	110	10
			46.68	0.02		03	56.9	0.6	0	< 2.2	< 1	10	5
			46.89	0.01		04	04.0	0.4	0	< 2.2	< 1	40	10

TABLE I—*continued*

Polarization %	±	p.a. o	θ "	p.a. o	z	Distance (Mpc)	Total size (kpc)	U_{min} (10^{56} erg)	B_{eq} (10^{-5} G)	5GHz Synch. lifetime (10^{4} yr)	Source 3C/4C
< 4											
8	1	173	2.3	71		580	5.9	< 36	> 4	< 82	346
< 15								< 11	> 3	< 150	
20	5	144	31.0	68	0.0917	520	71	3.5	6.1	50	388
-								170	1.7	340	
< 22								< 0.5	> 4	< 85	
< 36								7.9	3.9	99	
-								140	1.9	290	
30	4	165	27.1	105	0.469	2100	190	< 560	> 3	< 150	411
< 40								< 12	> 2	< 290	
< 40								5000	1.6	380	
12	3	130						< 220	> 7	< 38	
16	2	146	23.1	141							427.1
13	2	56									
see map			50	25	0.1025	570	150	800	2	300	433
-								240	1.2	580	
10	3	120	12	81	0.767	2970	99	< 1700	> 3	< 150	434
< 20								< 1000	> 5	< 110	
					0.323	1570	70	< 380	> 2	< 200	434
								< 240	> 3	< 150	
< 7			1.0	160							454.1
< 6			4.9	36	0.28	1400	26	< 100	> 11	< 21	460
< 13								< 71	> 7	< 37	
< 25			32	159	0.632	2600	250	< 310	> 4	< 92	467
< 6								< 260	> 8	< 30	
-								550	2.0	270	
											25.03
					0.0366	210	40	< 0.07	> 5	< 70	35.03
								23	1.3	510	
			15	23	1.27	4000	130	< 560	> 7	< 37	24.23
								< 15	> 2	< 190	
								< 170	> 8	< 34	

Components which are unresolved in at least one dimension can be given only upper limits for the energy (15) and half-life (17) and lower limits for the magnetic field (16).

3. OPTICAL IDENTIFICATIONS

The optical fields around most of the sources in the 3C catalogue have been studied in some detail, and in many cases the optical positions of the most likely identification have been measured with high accuracy. The optical positions plotted on the maps are those with the smallest estimated errors, or in some cases the means of two measurements quoting similar, small errors.

In 13 cases there are compact central radio components which unambiguously define the optical identifications. In all these cases good agreement is found between the radio components and optical nuclei. A detailed comparison of the positions may be used to test the reliability of the estimates of positional accuracy. A similar analysis was carried out for the optical sources included in the astrometric observations of Ryle & Elsmore (1973). In the latter cases the positions were derived from the variation of measured phase between the different elements of the interferometer, giving accuracies of $\approx 0''{\cdot}03$. The discrepancies in the relative optical and radio positions were therefore predominantly due either to the errors in the optical positions, or to non-coincidence of the optical and radio sources.

In the present cases, where the nuclear components usually provide only a few per cent of the total flux density, the positions were necessarily measured from the contour maps; the lower weight attached to observations at the larger baselines means that the accuracies are limited to one-tenth to one-twentieth of the beamwidth, i.e. $0''{\cdot}1$–$0''{\cdot}2$ in α and $0''{\cdot}1$–$0''{\cdot}2 \operatorname{cosec} \delta$ in δ. The accuracy is nevertheless still usually better than that of the optical positions, and a comparison of the rms differences obtained by several optical observers is given in Table II. In all cases the differences are consistent with the estimated errors in the optical and radio positions.

Gunn & Longair (1975) show photographs of the fields of 3C 6·1, 68·2, 123, 427·1, 433, 434, 454·1 and 560.

TABLE II

Authors	No. of sources	Rms difference (″) α	δ
Argue & Kenworthy (AK 1972)	4	0·34	0·21
Murray, Tucker & Clements (MTC 1971)	4	0·43	0·19
Wills, Wills & Douglas (WWD 1973)	2	0·35	0·38
Griffin (G 1963)	2	0·08	0·51
Véron* (SVW 1965; V 1966, 1968; Véron & Véron 1973)	9	0·71	0·84
Barbieri, Capaccioli, (Ganz) & Pinto (BCP 1970; BCGP 1972)	6	1·09	0·73
Lü & Fredrick (1967)	3	1·17	2·79

* The position given for 3C 47 (SVW) has not been included since it is 6″ from the radio position.

4. NOTES ON INDIVIDUAL SOURCES

3C 9

The present results and interferometric observations at 408 and 2695 MHz (Clark & Miley 1969) give spectral indices between 408 MHz and 5 GHz of $0{\cdot}98 \pm 0{\cdot}04$ for the Sf and $1{\cdot}36 \pm 0{\cdot}05$ for the Np component. The spectrum of the latter must flatten at lower frequencies or else its flux density extrapolated to 60 MHz would be greater than the total flux density of the source (Fig. 3(a)). The total spectrum shows a break at 200 ± 50 MHz which is probably due to this break in the spectrum of the Np component, and the parameters derived for this component are on the assumption that synchrotron losses become important at 200 MHz. The actual age of the component (assuming equipartition of energy between magnetic field and relativistic electrons) is then 6×10^5 yr.

3C 67

The separation of the components ($2''{\cdot}00 \pm 0''{\cdot}08$) has been derived from the visibility function, assuming the source to be double. The position (V) of the 18^m galaxy is $0''{\cdot}4 \pm 1''$ from the radio centre. No map is shown.

3C 123

The polarized structure of this source is complex. The peak of the Np component is 5 ± 1 per cent polarized in p.a. 148°, the tail to the E has 12 ± 2 per cent polarization in p.a. 89° while the tail to the S is less than 4 per cent polarized. The polarization in the low surface brightness region of the Sf component reaches 15 ± 5 per cent in three places, each with a different p.a. (129°, 24°, 151°). The polarized structure bears little relation to the structure of the total intensity, as has also been found in the extended, low brightness regions of Cygnus A (Hargrave & Ryle 1974).

3C 196

The present 5 GHz results, taken with interferometric observations at 2·7 GHz (Hogg 1969; Bash 1968a) and 408 MHz (Wilkinson 1972), give a spectral index of $0{\cdot}85 \pm 0{\cdot}08$ for the preceding and $0{\cdot}70 \pm 0{\cdot}08$ for the following component. Long baseline interferometry at 1423 MHz (Wilkinson 1972) shows that there is structure smaller than $0''{\cdot}4$ in each of the two major components contributing half the flux density of the source.

3C 207

The total spectrum is concave above 1 GHz and the sum of the flux densities of the outer components at 5 GHz lies on the extrapolation of the low frequency spectrum (Fig. 3(b)). This implies that the unresolved central component has a flat spectrum and its contribution to the total flux density is negligible below 1 GHz.

This conclusion is supported by the visibility function obtained by Bash (1968b) at 2·7 GHz, which is consistent with a triple source similar to that mapped at 5 GHz, with $0{\cdot}55 \pm 0{\cdot}07$ fu in the central component. The spectral index of the latter between 2·7 and 5·0 GHz is then $0{\cdot}1 \pm 0{\cdot}3$.

3C 236

The separation of the components of this compact source ($0''{\cdot}78 \pm 0''{\cdot}03$) has been derived from the visibility function, assuming that the source is double. No map is shown.

3C 254

The position (G) of the suggested identification, a quasar, is unusual in that it lies 1″·6±0″·5 from the following component and 12″ from the preceding component. However, the former is unlikely to be a component of the type often found to be coincident with a quasar, not only because of the discrepancy between the radio and optical positions, but also because it is extended and does not have a

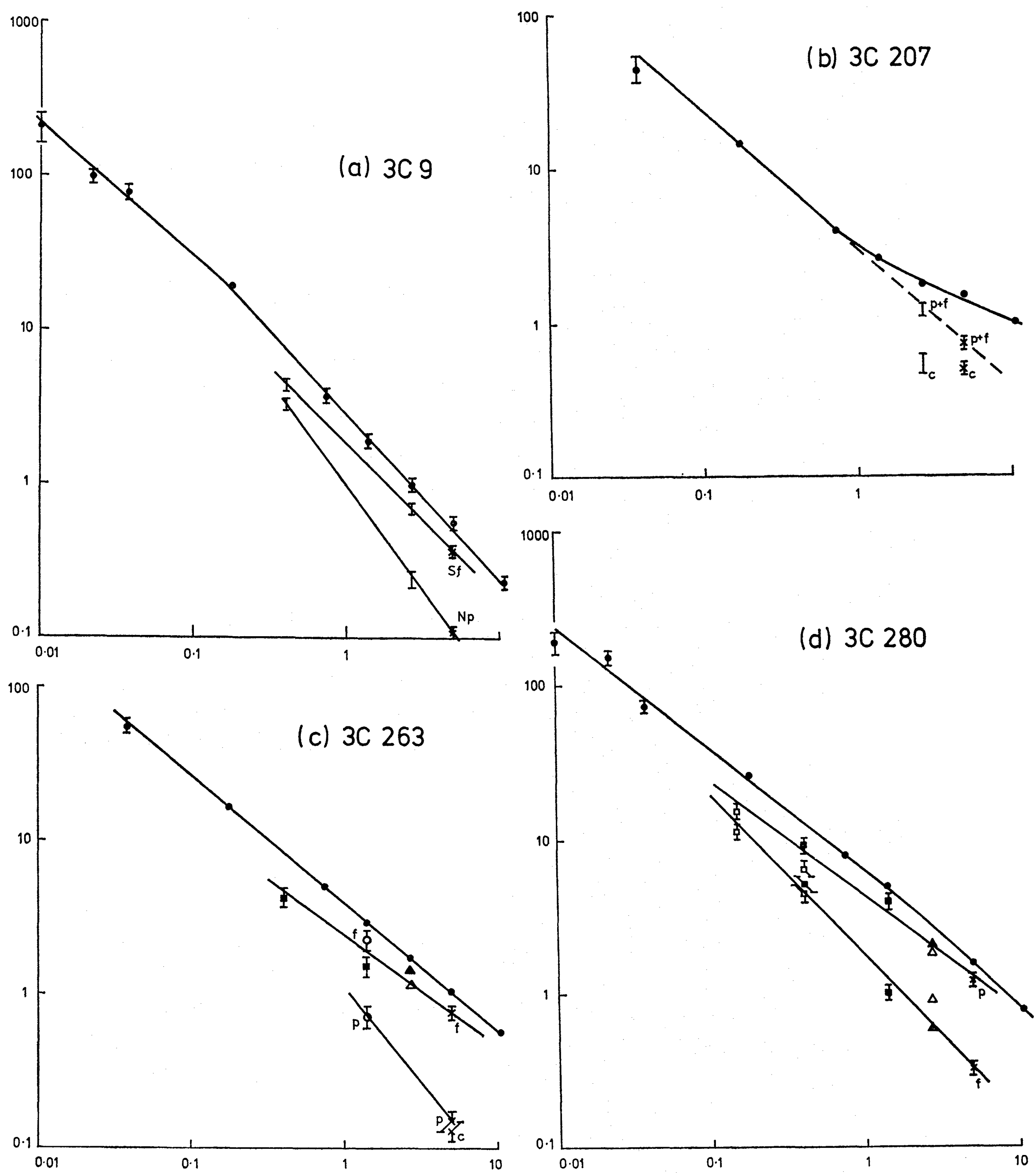

Fig. 3.

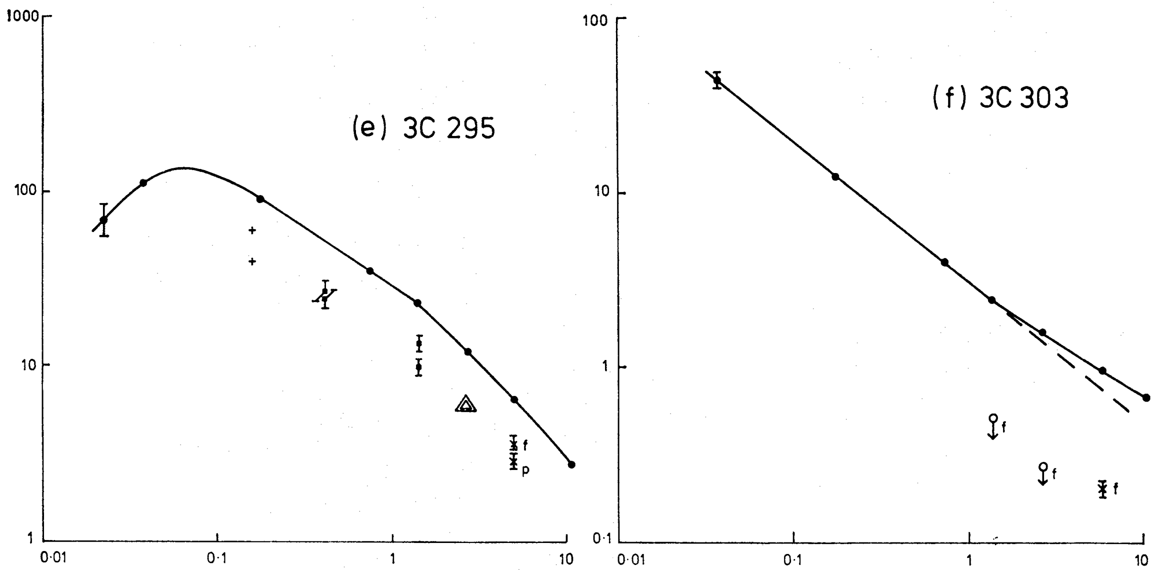

FIG. 3. *The spectra of six sources discussed in the text. The total spectrum of each source is defined by the flux densities given by Kellermann & Pauliny-Toth* (1973) (10·7 *GHz*), *Kellermann* et al. (1969) (5, 2·7, 1·4 *GHz*, 750, 178, 38 *MHz*), *Roger* et al. (1969) *and Roger* et al. (1973) (22·25 *MHz*), *and Bridle & Purton* (1968) (10·03 *MHz*). *Flux densities at frequencies below* 200 *MHz have been normalized to the scale defined by Roger* et al. (1973). *Flux density of components are from:* ×, 5-*km telescope;* ○, *Cambridge One-Mile Telescope;* ▲, *Bash* (1968*a*)*;* △, *Hogg* (1969) *or Clark & Hogg* (1966)*;* ■, *Wilkinson* (1972)*;* □, *Wraith* (1972)*;* +, *Anderson* et al. (1965). *Unlabelled error bars for* 3*C* 9 *are from Clark & Miley* (1969)*; and for* 3*C* 207 *are derived from observations by Bash* (*see text*). *The error bars on the flux densities from Wraith and from Wilkinson are* ±14 *per cent, the rms difference in flux density between sources observed by Stannard, Wraith & Wilkinson at* 408 *MHz* (*Wilkinson* 1972). *The flux density of the preceding* (*p*), *following* (*f*) *and central* (*c*) *components are marked where they may be measured unambiguously. The abscissae are marked in GHz, the ordinates in fu.*

flat spectrum ($\alpha_{2\cdot7}^{5\cdot0}$ = 1·0 ± 0·2). There is also no emission > 20 mfu from the region east of this component which might constitute a third component of the source.

The Sky Survey prints show no other possible identifications in the field, which is at high galactic latitude (b = 66°).

3C 263

The present results at 5 GHz, One-Mile Telescope observations at 1·4 GHz, and interferometric results at 2·7 GHz (Hogg 1969; Bash 1968a), 408 and 1423 MHz (Wilkinson 1972) give a spectral index of 0·68 ± 0·08 for the compact following component (Fig. 3(c)). There is no evidence for the concave curvature of the spectrum of this component suggested by Wilkinson.

The flux density of the preceding component at 1·4 GHz as measured by the One-Mile Telescope is 0·7 ± 0·1 fu, giving a spectral index between 1·4 and 5 GHz of 1·2 ± 0·2 (Fig. 3(c)).

3C 268.3

The separation of the components of this compact source (1″·28 ± 0″·04) has been derived from the visibility function. KSK identify this source with a 19^{m} galaxy in a cluster, which lies 1″·3 ± 1″ from the mean position given here. No map is shown.

3C 277.1

The visibility function of this compact source ($\approx 1''\cdot 3$) is not fitted well by either a simple double or a Gaussian distribution of emission. The peak of radio emission coincides with the optical position (AK, MTC) of the 18^m quasar. No map is shown.

3C 280

Interferometric observations at 151 MHz (Wraith 1972), 408 MHz (Wraith 1972; Wilkinson 1972), 1423 MHz (Wilkinson 1972) and 2695 MHz (Bash 1968a) and the present 5 GHz results show that the two components of this source have significantly different spectral indices: $0\cdot 69 \pm 0\cdot 08$ for the preceding component and $1\cdot 04 \pm 0\cdot 08$ for the following (Fig. 3(d)).

Scintillation measurements at 81·5 MHz (Readhead & Hewish 1974) show a component of $1''\cdot 0 \pm 0''\cdot 3$ half-power width, of flux density 23 ± 10 fu. The flux density of the unresolved following component at 81·5 MHz (extrapolated from its high frequency spectrum) is 22 ± 4 fu, consistent with it being the scintillating component.

3C 295

The present 5 GHz results, together with interferometric observations at 159 MHz (Anderson, Palmer & Rowson 1962), 408 MHz and 1423 MHz (Wilkinson 1972) and 2695 (Clark & Hogg 1966), show that the two components have similar spectral indices ($\approx 0\cdot 8$) between 150 MHz and 5 GHz. The total spectrum has a gradual turnover at 70 ± 15 MHz which is unlikely to be due to free-free absorption in our Galaxy because of the high galactic latitude of the source ($b = +61°$). This turnover must occur in the spectra of both components as the flux density at 50 MHz is less than the extrapolated flux density of either component (Fig. 3(a)).

The 5 km visibility function gives component sizes of $0''\cdot 7$ and $1''\cdot 0$, but long baseline interferometry at 1·4 and 2·7 GHz (Donaldson *et al.* 1969) indicates that there is also smaller scale structure present. Taking an 'average' size of $0''\cdot 5$ for both components of the source, the equipartition field of each component is about 4×10^{-4} G. In this field both components become optically thick at about 70 MHz which is in good agreement with the observed turnover frequency.

The total spectrum steepens abruptly near 1·4 GHz, where the spectral index increases from 0·7 to 1·0, and it becomes increasingly steep at higher frequencies. If this break is interpreted in terms of synchrotron losses the age of the components is only 10^5 yr, not much greater than the light travel time of the components from the central galaxy (5×10^4 yr).

3C 303

The identification of this source is in some doubt. Neither of two possible candidates, a 17^m galaxy measured by Véron (1966) and a 16^m galaxy $15''$ to the east, appears to be near the centre of the source.

The 5 GHz observations suggest that there is some low-brightness emission from this source. In addition the spectrum is concave (Fig. 3(f)) and this curvature may be caused by the relatively flat spectrum of the following component ($\alpha < 0\cdot 15$).

The polarization of the preceding component is unusually strong.

3C 433

This source has a very unusual shape, and relatively strong linear polarization (10–35 per cent). Mackay (1969) notes that the low-brightness region to the NE extends for some 70″, contributing 10 per cent of the flux at 1407 MHz. There appears to be no significant small-scale structure (<2″) either at 5 GHz, or at 81·5 MHz from scintillation data (Readhead & Hewish 1974).

3C 454.1

The separation of the components of this compact source (1″·0 ± 0″·1) has been derived from the visibility function. There is no optical identification (GL). No map is shown.

4C 25.03

A 17^{m} galaxy (Olsen 1970) lies 36″ SW of the radio source. There is no radio component having $S > 20$ mfu within 90″ on the other side of the galaxy, and it is unlikely that the galaxy is related to the source. The parameters for this source are derived from the visibility function and no map is shown.

5. CONCLUSIONS

These observations of extragalactic sources do not yet form a statistically complete sample, since their selection was not on a uniform basis. Further observations designed to provide well-defined samples are in progress and discussions of astrophysical results will follow in later papers.

ACKNOWLEDGMENTS

These observations were only possible through the efforts of many members of the Observatory staff, to whom we express our thanks.

SNH acknowledges the receipt of a grant from the Northern Ireland Department of Education.

Mullard Radio Astronomy Observatory, Cavendish Laboratory, Cambridge

REFERENCES

Anderson, B., Palmer, H. P. & Rowson, B., 1962. *Nature*, **195**, 165.
Argue, A. N. & Kenworthy, C. M., 1972. *Mon. Not. R. astr. Soc.*, **160**, 197.
Barbieri, C., Capaccioli, M., Ganz, R. & Pinto, G., 1972. *Astr. J.*, **77**, 444.
Barbieri, C., Capaccioli, M. & Pinto, G., 1970. *Mem. Soc. astr. Ital.*, **41**, 459.
Bash, F. N., 1968a. *Astrophys. J. Suppl.*, **16**, 373.
Bash, F. N., 1968b. *Astrophys. J.*, **152**, 375.
Bennett, A. S., 1962. *Mem. R. astr. Soc.*, **68**, 163.
Branson, N. J. B. A., Elsmore, B., Pooley, G. G. & Ryle, M., 1972. *Mon. Not. R. astr. Soc.*, **156**, 377.
Bridle, A. H. & Purton, C. R., 1968. *Astr. J.*, **73**, 717.
Burbidge, E. M., Burbidge, G. R., Solomon, P. M. & Strittmatter, P. A., 1971. *Astrophys. J.*, **170**, 233.
Clark, B. G. & Hogg, D. E., 1966. *Astrophys. J.*, **145**, 21.
Clark, B. G. & Miley, G. K., 1969. *Astrophys. Letters*, **4**, 207.

Donaldson, W., Miley, G. K., Palmer, H. P. & Smith, H., 1969. *Mon. Not. R. astr. Soc.*, **146**, 213.
Edge, D. O., Shakeshaft, J. R., McAdam, W. B., Baldwin, J. E. & Archer, S., 1959. *Mem. R. astr. Soc.*, **68**, 37.
Griffin, R. F., 1963. *Astr. J.*, **68**, 421.
Gunn, J. E. & Longair, M. S., 1975. *Mon. Not. R. astr. Soc.*, **170**, 121.
Hargrave, P. J. & Ryle, M., 1974. *Mon. Not. R. astr. Soc.*, **166**, 305.
Hinder, R. A. & Ryle, M., 1971. *Mon. Not. R. astr. Soc.*, **154**, 229.
Hogg, D. E., 1969. *Astrophys. J.*, **155**, 1099.
Hunstead, R. W., 1971. *Mon. Not. R. astr. Soc.*, **152**, 277.
Kapahi, V. K., Gopal-Krishna & Joshi, M. N., 1974. *Mon. Not. R. astr. Soc.*, **167**, 299.
Kellermann, K. I. & Pauliny-Toth, I. I. K., 1973. *Astr. J.*, **78**, 828.
Kellermann, K. I., Pauliny-Toth, I. I. K. & Williams, P. J. S., 1969. *Astrophys. J.*, **157**, 1.
Kristian, J., Sandage, A. & Katem, B., 1974. *Astrophys. J.*, **191**, 43.
Longair, M. S., 1965. *Mon. Not. R. astr. Soc.*, **129**, 419.
Lü, P. K. & Fredrick, L. W., 1967. *Astrophys. J.* (*Letters*), **150**, L71.
Mackay, C. D., 1969. *Mon. Not. R. astr. Soc.*, **145**, 31.
Murray, C. A., Tucker, R. H. & Clements, E. D., 1971. *R. Obs. Bull.*, **162**.
Oemler, A., Gunn, J. E. & Oke, J. B., 1972. *Astrophys J.* (*Letters*), **176**, L47.
Olsen, E. T., 1970. *Astr. J.*, **75**, 764.
Pilkington, J. D. H. & Scott, P. F., 1965. *Mem. R. astr. Soc.*, **69**, 183.
Readhead, A. C. S. & Hewish, A., 1974. *Mem. R. astr. Soc.*, **78**, 1.
Roger, R. S., Bridle, A. H. & Costain, C. H., 1973. *Astr. J.*, **78**, 1030.
Roger, R. S., Costain, C. H. & Lacey, J. D., 1969. *Astr. J.*, **74**, 366.
Ryle, M., 1972. *Nature*, **239**, 435.
Ryle, M. & Elsmore, B., 1973. *Mon. Not. R. astr. Soc.*, **164**, 223.
Sandage, A., 1966. *Astrophys. J.*, **145**, 1.
Sandage, A., 1967. *Astrophys. J.* (*Letters*), **150**, L9.
Sandage, A., Véron, P. & Wyndham, J. D., 1965. *Astrophys. J.*, **142**, 1307.
Spinrad, H. & Smith, H. E., 1974. In preparation.
Spinrad, H., Smith, H. E., Hunstead, R. & Ryle, M., 1974. In preparation.
Véron, P., 1966. *Astrophys. J.*, **144**, 861.
Véron, P., 1968. *Ann. Astrophys.*, **31**, 483.
Véron, P. & Véron, M. P., 1973. *Astr. Astrophys.*, **28**, 319.
Wilkinson, P. N., 1972. *Mon. Not. R. astr. Soc.*, **160**, 305.
Wills, B. J., Wills, D. & Douglas, J. N., 1973. *Astr. J.*, **78**, 521.
Wlérick, G., Lelièvre, G. & Véron, P., 1971. *Astr. Astrophys.*, **11**, 142.
Wraith, P. K., 1972. *Mon. Not. R. astr. Soc.*, **160**, 283.